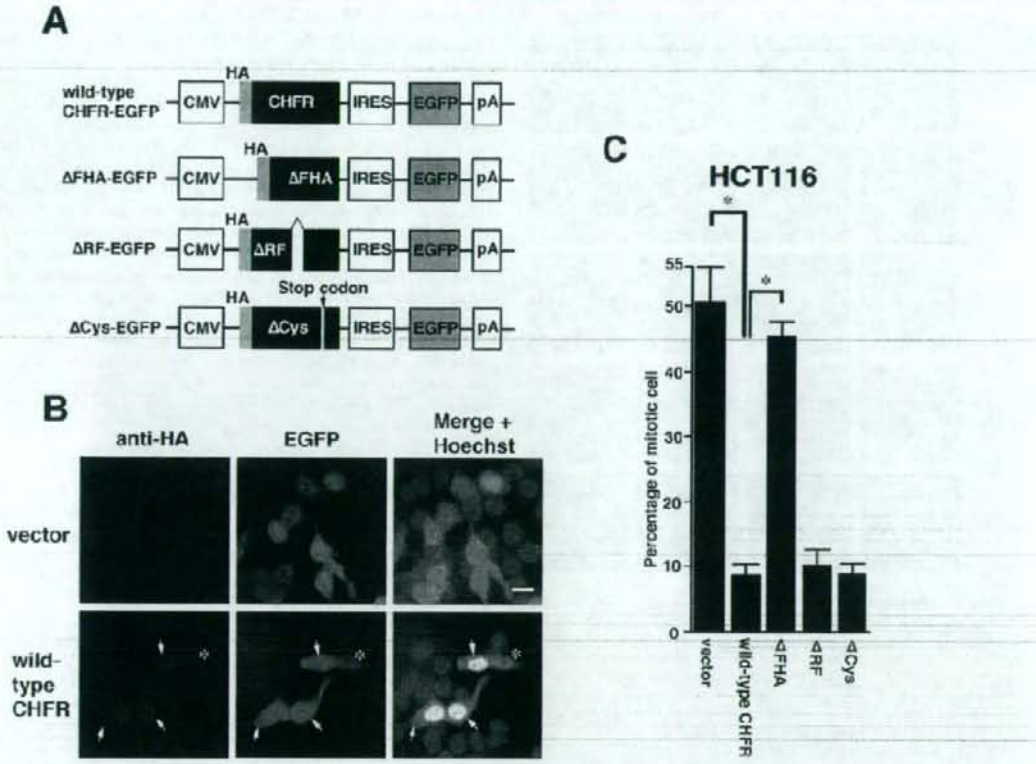

Figure 5. Checkpoint assay of the wild type and mutant forms of the CHFR protein. (A) Schematic representation of the bicistronic vectors used to express the indicated CHFR products. (B) Validation of the positive correlation between the anti-HA antibody immunoreactivity and EGFP expression profiles. Cells that were positive for both are denoted by arrows. Cells that were positive for the anti-HA antibody, but not for EGFP, are highlighted by an asterisk. (C) Mitotic checkpoint analysis of HCT116 cells after the introduction of an empty vector, wild-type-EGFP, ΔFHA-EGFP, ΔRF-EGFP or ΔCys-EGFP. Asterisks indicate statistical significance ($p<0.05$).
doi:10.1371/journal.pone.0001776.g005

proliferative effect can be explained with the binding of new candidates and CHFR. These information will help us to gain further insights in understanding how a functional loss of this gene leads to increased cell proliferation during gastrointestinal carcinogenesis.

Table 1. Summary of the functional properties of wild-type, ΔFHA, ΔRF and ΔCys CHFR proteins.

	Wild type CHFR	ΔFHA	ΔRF	ΔCys
Anti-proliferative effects	Yes	No	Yes	Yes
E3 ligase activity	Yes	Yes	No	No
Cellular localization	Nucleus	Nucleus	Nucleus	Nucleus
Checkpoint function	Yes	No	Yes	Yes

doi:10.1371/journal.pone.0001776.t001

Acknowledgments

We thank Noriyuki Matsuda and Yukiko Yoshida (Tokyo Metropolitan Institute of Medical Sciences, Tokyo, Japan), Mitsuyasu Kato and Hiroyuki Suzuki (University of Tsukuba, Institute of Basic Medical Sciences) for their helpful advice and discussions, providing the FLAG-Ubiquitin expression plasmid. We also thank Hiroshi Tazawa, Naoto Tsuchiya, Daisuke Maeda and Tasuku Suzuki (Biochemistry Division and ADP-ribosylation in Oncology project in the National Cancer Center Research Institute) for technical help and discussions throughout this study. We are grateful to Hideko Fukuda (National Institute of Environmental Health Studies, Tsukuba, Japan) for her support and encouragement throughout this project.

Author Contributions

Conceived and designed the experiments: TF. Performed the experiments: TF YK. Analyzed the data: TF YK. Contributed reagents/materials/analysis tools: TF. Wrote the paper: TF. Other: Supervised the experiments and study: HN.

References

1. Scolnick DM, Halazonetis TD (2000) Chfr defines a mitotic stress checkpoint that delays entry into metaphase. Nature 406: 430–435.
2. Hamilton JP, Sato F, Greenwald BD, Suntharalingam M, Krasna MJ, et al. (2006) Promoter methylation and response to chemotherapy and radiation in esophageal cancer. Clin Gastroenterol Hepatol 4: 701–708.
3. Koga Y, Kitajima Y, Miyoshi A, Sato K, Sato S, et al. (2006) The significance of aberrant CHFR methylation for clinical response to microtubule inhibitors in gastric cancer. J Gastroenterol 41: 133–139.
4. Satoh A, Toyota M, Itoh F, Sasaki Y, Suzuki H, et al. (2003) Epigenetic inactivation of CHFR and sensitivity to microtubule inhibitors in gastric cancer. Cancer Res 63: 8606–8613.
5. Yanokura M, Banno K, Kawaguchi M, Hirao N, Hirasawa A, et al. (2007) Relationship of aberrant DNA hypermethylation of CHFR with sensitivity to taxanes in endometrial cancer. Oncol Rep 17: 41–48.
6. Yoshida K, Hamai Y, Suzuki T, Sanada Y, Oue N, et al. (2006) DNA methylation of CHFR is not a predictor of the response to docetaxel and paclitaxel in advanced and recurrent gastric cancer. Anticancer Res 26: 49–54.
7. Summers MK, Bothos J, Halazonetis TD (2005) The CHFR mitotic checkpoint protein delays cell cycle progression by excluding Cyclin B1 from the nucleus. Oncogene 24: 2589–2598.
8. Dasika GK, Lin SC, Zhao S, Sung P, Tomkinson A, et al. (1999) DNA damage-induced cell cycle checkpoints and DNA strand break repair in development and tumorigenesis. Oncogene 18: 7883–7899.
9. Durocher D, Jackson SP (2002) The FHA domain. FEBS Lett 513: 58–66.
10. Williams BR, Mirzoeva OK, Morgan WF, Lin J, Dunnick W, et al. (2002) A murine model of Nijmegen breakage syndrome. Curr Biol 12: 648–653.
11. Jongmans W, Vuillaume M, Chrzanowska K, Smeets D, Sperling K, et al. (1997) Nijmegen breakage syndrome cells fail to induce the p53-mediated DNA damage response following exposure to ionizing radiation. Mol Cell Biol 17: 5016–5022.
12. Vahteristo P, Tamminen A, Karvinen P, Eerola H, Eklund C, et al. (2001) p53, CHK2, and CHK1 genes in Finnish families with Li-Fraumeni syndrome: further evidence of CHK2 in inherited cancer predisposition. Cancer Res 61: 5718–5722.
13. Hirao A, Cheung A, Duncan G, Girard PM, Elia AJ, et al. (2002) Chk2 is a tumor suppressor that regulates apoptosis in both an ataxia telangiectasia mutated (ATM)-dependent and an ATM-independent manner. Mol Cell Biol 22: 6521–6532.
14. Takai H, Naka K, Okada Y, Watanabe M, Harada N, et al. (2002) Chk2-deficient mice exhibit radioresistance and defective p53-mediated transcription. Embo J 21: 5195–5205.
15. Brandes JC, van Engeland M, Wouters KA, Weijenberg MP, Herman JG (2005) CHFR promoter hypermethylation in colon cancer correlates with the microsatellite instability phenotype. Carcinogenesis 26: 1152–1156.
16. Homma N, Tamura G, Honda T, Jin Z, Ohmura K, et al. (2005) Hypermethylation of Chfr and hMLH1 in gastric noninvasive and early invasive neoplasias. Virchows Arch 446: 126–126.
17. Bertholon J, Wang Q, Faleur N, Verny C, Audair J, et al. (2003) Chfr inactivation is not associated to chromosomal instability in colon cancers. Oncogene 22: 8956–8960.
18. Corn PG, Summers MK, Fogt F, Virmani AK, Gazdar AF, et al. (2003) Frequent hypermethylation of the 5' CpG island of the mitotic stress checkpoint gene Chfr in colorectal and non-small cell lung cancer. Carcinogenesis 24: 47–51.
19. Toyota M, Sasaki Y, Satoh A, Ogi K, Kikuchi T, et al. (2003) Epigenetic inactivation of CHFR in human tumors. Proc Natl Acad Sci U S A 100: 7818–7823.
20. Visintin R, Prinz S, Amon A (1997) CDC20 and CDH1: a family of substrate-specific activators of APC-dependent proteolysis. Science 278: 460–463.
21. Yu X, Minter-Dykhouse K, Malureanu L, Zhao WM, Zhang D, et al. (2005) Chfr is required for tumor suppression and Aurora A regulation. Nat Genet 37: 401–406.
22. Kang D, Chen J, Wong J, Fang G (2002) The checkpoint protein Chfr is a ligase that ubiquitinates Plk1 and inhibits Cdc2 at the G2 to M transition. J Cell Biol 156: 249–259.
23. Strebhardt K, Ullrich A (2006) Targeting polo-like kinase 1 for cancer therapy. Nat Rev Cancer 6: 321–330.
24. Nigg EA (2001) Mitotic kinases as regulators of cell division and its checkpoints. Nat Rev Mol Cell Biol 2: 21–32.
25. Bischoff JR, Anderson L, Zhu Y, Mossie K, Ng L, et al. (1998) A homologue of Drosophila aurora kinase is oncogenic and amplified in human colorectal cancers. Embo J 17: 3052–3065.
26. Zhou H, Kuang J, Zhong L, Kuo WL, Gray JW, et al. (1998) Tumour amplified kinase STK15/BTAK induces centrosome amplification, aneuploidy and transformation. Nat Genet 20: 189–193.
27. Ogi K, Toyota M, Mita H, Satoh A, Kashima L, et al. (2005) Small interfering RNA-induced CHFR silencing sensitizes oral squamous cell cancer cells to microtubule inhibitors. Cancer Biol Ther 4: 773–780.
28. Chaturvedi P, Sudakin V, Bobiak ML, Fisher PW, Matthew MR, et al. (2002) Chfr regulates a mitotic stress pathway through its RING-finger domain with ubiquitin ligase activity. Cancer Res 62: 1797–1801.
29. Bothos J, Summers MK, Venere M, Scolnick DM, Halazonetis TD (2003) The Chfr mitotic checkpoint protein functions with Ubc13-Mms2 to form Lys63-linked polyubiquitin chains. Oncogene 22: 7101–7107.
30. Fukuda T, Mishina Y, Walker MP, DiAugustine RP (2005) Conditional transgenic system for mouse aurora a kinase: degradation by the ubiquitin proteasome pathway controls the level of the transgenic protein. Mol Cell Biol 25: 5270–5281.
31. Wang W, Malcolm BA (1999) Two-stage PCR protocol allowing introduction of multiple mutations, deletions and insertions using QuikChange Site-Directed Mutagenesis. Biotechniques 26: 680–682.
32. Koinuma D, Shinozaki M, Komuro A, Goto K, Saitoh M, et al. (2003) Arkadia amplifies TGF-beta superfamily signalling through degradation of Smad7. Embo J 22: 6458–6470.
33. Daniels MJ, Marson A, Venkitaraman AR (2004) PML bodies control the nuclear dynamics and function of the CHFR mitotic checkpoint protein. Nat Struct Mol Biol 11: 1114–1121.
34. Martinez R, Setien F, Voelter C, Casado S, Quesada MP, et al. (2007) CpG island promoter hypermethylation of the pro-apoptotic gene caspase-8 is a common hallmark of relapsed glioblastoma multiforme. Carcinogenesis.
35. Tokumaga E, Oki E, Nishida K, Koga T, Yoshida R, et al. (2006) Aberrant hypermethylation of the promoter region of the CHFR gene is rare in primary breast cancer. Breast Cancer Res Treat 97: 199–203.
36. Littlepage LE, Ruderman JV (2002) Identification of a new APC/C recognition domain, the A box, which is required for the Cdh1-dependent destruction of the kinase Aurora-A during mitotic exit. Genes Dev 16: 2274–2285.
37. Crane R, Kloepfer A, Ruderman JV (2004) Requirements for the destruction of human Aurora-A. J Cell Sci 117: 5975–5983.
38. Kawai H, Wiederschain D, Yuan ZM (2003) Critical contribution of the MDM2 acidic domain to p53 ubiquitination. Mol Cell Biol 23: 4939–4947.
39. Kawai H, Lopez-Pajares V, Kim MM, Wiederschain D, Yuan ZM (2007) RING domain-mediated interaction is a requirement for MDM2's E3 ligase activity. Cancer Res 67: 6026–6030.
40. Takai R, Matsuda N, Nakano A, Hasegawa K, Akimoto C, et al. (2002) EL5, a rice N-acetylchitooligosaccharide elicitor-responsive RING-H2 finger protein, is a ubiquitin ligase which functions in vitro in co-operation with an elicitor-responsive ubiquitin-conjugating enzyme, OsUBC5b. Plant J 30: 447–455.
41. Matsuda N, Suzuki T, Tanaka K, Nakano A (2001) Rma1, a novel type of RING finger protein conserved from Arabidopsis to human, is a membrane-bound ubiquitin ligase. J Cell Sci 114: 1949–1957.
42. Matsuda N, Kitami T, Suzuki T, Mizuno Y, Hattori N, et al. (2006) Diverse effects of pathogenic mutations of Parkin that catalyze multiple monoubiquitylation in vitro. J Biol Chem 281: 3204–3209.
43. Privette LM, Gonzalez ME, Ding L, Kleer CG, Peuy EM (2007) Altered expression of the early mitotic checkpoint protein, CHFR, in breast cancers: implications for tumor suppression. Cancer Res 67: 6064–6074.
44. Morioka Y, Hibi K, Sakai M, Koike M, Fujiwara M, et al. (2006) Aberrant methylation of the CHFR gene is frequently detected in non-invasive colorectal cancer. Anticancer Res 26: 4267–4270.

Carcinogenesis vol.29 no.4 pp.834–839, 2008
doi:10.1093/carcin/bgn051
Advance Access publication February 17, 2008

Protective versus promotional effects of white tea and caffeine on PhIP-induced tumorigenesis and β-catenin expression in the rat

Rong Wang[1], W.Mohaiza Dashwood[1], Christiane V.Löhr[2], Kay A.Fischer[2], Clifford B.Pereira[3], Mandy Louderback[1], Hitoshi Nakagama[4], George S.Bailey[1], David E.Williams[1,5] and Roderick H.Dashwood[1,5,*]

[1]Linus Pauling Institute, [2]College of Veterinary Medicine and [3]Department of Statistics, Oregon State University, Corvallis, OR 97331, USA, [4]Biochemistry Division, National Cancer Center Research Institute, 1-1, Tsukiji 5-chome, Chuo-ku, Tokyo 104-0045, Japan and [5]Department of Environmental and Molecular Toxicology, Oregon State University, Corvallis, OR 97331, USA

*To whom correspondence should be addressed. Tel: +1 541 737 5086; Fax: +1 541 737 5077; Email: Rod.Dashwood@oregonstate.edu

A 1 year carcinogenicity bioassay was conducted in rats treated with three short cycles of 2-amino-1-methyl-6-phenylimidazo[4,5-*b*]pyridine (PhIP)/high-fat (HF) diet, followed by 2% white tea (wt/vol), 0.05% epigallocatechin-3-gallate (EGCG) or 0.065% caffeine as sole source of fluid intake. Thirty-two percent of the PhIP/HF controls survived to 1 year, compared with 50, 48.7 and 18.2% in groups given white tea, EGCG and caffeine, respectively. After 1 year, PhIP/HF controls had tumors in the colon, skin, small intestine, Zymbal's gland, salivary gland and pancreas. For all sites combined, excluding the colon, tumor incidence data were as follows: PhIP/HF 69.5%, PhIP/HF + EGCG 48.7%, PhIP/HF + white tea 46.9% and PhIP/HF + caffeine 13.3%. Unexpectedly, a higher incidence of colon tumors was detected in rats post-treated with white tea (69%) and caffeine (73%) compared with the 42% incidence in PhIP/HF controls. In the colon tumors, β-catenin mutations were detected at a higher frequency after caffeine posttreatment, and there was a shift toward more tumors harboring substitutions of Gly34 with correspondingly high protein and messenger RNA expression seen for both β-catenin and c-Myc. c-Myc expression exhibited concordance with tumor promotion, and there was a concomitant increase in cell proliferation versus apoptosis in colonic crypts. A prior report described suppression of PhIP-induced colonic aberrant crypts by the same test agents, but did not incorporate a HF diet. These findings are discussed in the context of epidemiological data which do not support an adverse effect of tea and coffee on colon tumor outcome—indeed, some such studies suggest a protective role for caffeinated beverages.

Introduction

It is now well established that human colorectal cancers contain mutations that stabilize the β-catenin protein, causing constitutive activation of β-catenin/T-cell factor (Tcf) signaling and overexpression of downstream targets, such as c-Myc, c-Jun and cyclin D1 (1). Similar findings have been reported in preclinical models of colon cancer. For example, carcinogen-induced rat colon tumors contain oncogenic mutants of β-catenin that are resistant to degradation via the phosphorylation/ubiquitination/proteosome pathway (2), and β-catenin stabilization constitutively activates c-*myc*, c-*jun* and *cyclin D1* expression in the corresponding tumors (3,4). However, the frequency and spectrum of β-catenin mutations depends on the dosing protocol employed. Continuous feeding of the heterocyclic amine 2-amino-1-methyl-6-phenylimidazo[4,5-*b*]pyridine (PhIP) produced colon tumors with high levels of β-catenin expression (5), and the tumors harbored mutations in either β-catenin or adenomatous polyposis coli (6). When dietary PhIP was given via three short cycles followed by a high-fat (HF) diet, β-catenin protein again was expressed at high levels, but only 55% of the colon tumors harbored β-catenin or adenomatous polyposis coli mutations (7). The spectrum and frequency of β-catenin mutations also can be influenced by post-initiation exposure to phytochemicals. For example, a higher proportion of tumors containing direct substitutions in critical Ser/Thr residues of the β-catenin protein was seen following treatment with indole-3-carbinol and chlorophyllin (3,4).

In the present investigation, we sought to test the post-initiation tumor-suppressing effects of white tea and two of its major constituents, namely caffeine and the polyphenolic compound epigallocatechin-3-gallate (EGCG), in rats treated with PhIP/HF diet. White tea is the least processed type of tea; leaves of *Camellia sinensis* contain polyphenols that undergo increasing oxidation in the conversion of white to green to oolong and finally to black tea (8). Prior studies with white tea showed (i) potent antimutagenic effects against PhIP and other heterocyclic amines in the *Salmonella* assay; (ii) inhibition of β-catenin/Tcf activity *in vitro*; (iii) suppression of intestinal polyps in the Apc^{min} mouse and (iv) protection against PhIP-induced colonic aberrant crypt foci (ACF) in the rat (8–12). In the present report, white tea and caffeine given post-initiation unexpectedly promoted rather than suppressed PhIP-induced colon tumors. Caffeine increased β-catenin and c-Myc expression, altered the spectrum and frequency of β-catenin mutations and augmented cell proliferation while inhibiting apoptosis in colonic crypts.

Abbreviations: ACF, aberrant crypt foci; BrdU, 5-bromo-2′-deoxyuridine; *Ctnnb1*, β-catenin gene (rat); EGCG, epigallocatechin-3-gallate; HF, high fat; mRNA, messenger RNA; PBS, phosphate-buffered saline; PCR, polymerase chain reaction; PhIP, 2-amino-1-methyl-6-phenylimidazo[4,5-*b*]pyridine; Tcf, T-cell factor.

Materials and methods

Test agents

PhIP was purchased from Toronto Research Chemicals (Ontario, Canada) and prepared as an 8 mg/ml solution in test vehicle (0.8% dimethylsulfoxide in milliQ water, adjusted to pH 3.5 with 0.1 N HCl). AIN-93G, AIN-93M and AIN-93G supplemented with 23% (wt/wt) hydrogenated vegetable oil (HF diet) were obtained from Dyets (Bethlehem, PA). Mutan White tea (referred to hereafter as 'white tea') was provided by Stash Tea Co. (Portland, OR). A solution of 2% (wt/vol) white tea was prepared by brewing loose leaf tea (2 g/100 ml) for 3 min in just-boiled 0.5% citric acid buffer (26 mM, pH 2.7). EGCG (TEAVIGO™, DSM Nutritional Products, Basel, Switzerland) and caffeine (Sigma–Aldrich, St Louis, MO) also were dissolved in 0.5% citric acid buffer, which enhances the stability of tea constituents compared with milliQ water alone. Solutions were prepared fresh every 2–3 days, and the stability of tea constituents was verified by high-performance liquid chromatography, as reported (8). 5-Bromo-2′-deoxyuridine (BrdU; Sigma–Aldrich) was prepared as a 20 mM solution in phosphate-buffered saline (PBS).

Animals and treatments

These studies received prior approval from Oregon State University Institutional Animal Care and Use Committee. Male F344 rats, 3–4 weeks of age, were purchased from the National Cancer Institute and housed in a ventilated, temperature-controlled room at 25°C with a 12 h light–dark cycle. After acclimatization to the basal diet (AIN-93G) for 3 days, rats were treated with three cycles of PhIP/HF diet using a protocol modified from Ubagai *et al.* (7). Specifically, PhIP (50 mg/kg) or vehicle alone was given by oral gavage every day for 2 weeks and rats were fed standard AIN-93G (low fat) diet, and this was followed by 4 weeks on AIN-93G HF diet, during which time no PhIP was administered (Figure 1A). After three such cycles of PhIP/HF treatment, rats were switched to standard AIN-93M diet for the remainder of the study. At this time, rats were randomly assigned to the various treatment groups, namely 2% white tea, 0.05% EGCG, 0.065% caffeine or citrate buffer alone (controls), administered as before (12) as sole source of drinking fluid. Test and vehicle groups initially comprised 40 and 10 rats each, respectively, and survival was followed until the study was terminated at 1 year. Rats were euthanized early due to one of the following signs of morbidity: (i) sudden loss of body weight,

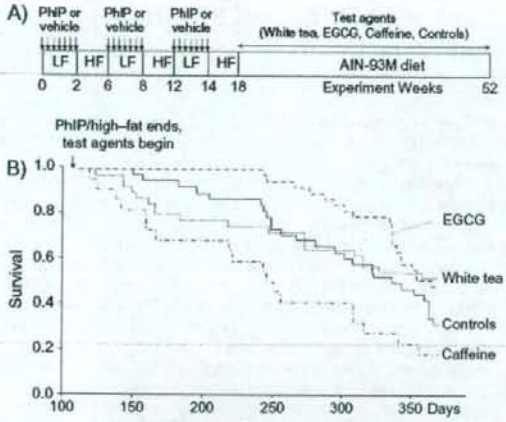

Fig. 1. Dosing protocol and survival curves of rats given PhIP/HF diet followed by white tea, EGCG or caffeine. **(A)** Male F344 rats were fed standard AIN-93G (low fat, LF) diet and given vehicle or PhIP (50 mg/kg) by oral gavage every day for 2 weeks, followed by 4 weeks on AIN-93G supplemented with 23% (wt/wt) hydrogenated vegetable oil (HF diet), during which time no PhIP was administered. After three such cycles, rats were switched to standard AIN-93M diet and given 2% white tea, 0.05% EGCG, 0.065% caffeine or citrate buffer alone (controls) as sole source of drinking fluid. **(B)** Survival curves of animals given PhIP/HF followed by white tea, EGCG or caffeine. The first sign of morbidity was at day 128 in the group post-treated with caffeine (dotted–dashed line). Data shown in the figure are cumulative and include animals that were euthanized before the study was terminated at 1 year.

appetite or fluid intake; (ii) bleeding in the stools over several days and (iii) overt discomfort and breathing difficulty or other signs of malaise. In all cases, rats were euthanized by CO_2 inhalation and a thorough necropsy was performed. One hour before killing, four rats in each group were selected at random to receive an intraperitoneal injection of 200 μmol BrdU/kg body wt.

Histopathology and immunohistochemistry

The following tissues were collected at necropsy: colon, small intestine, pancreas, prostate, lung, liver, kidney, bladder, skin and Zymbal's gland. The colon and small intestine were cleaned with cold PBS and opened longitudinally so as to record the position and size of tumors. Small tumors (<10 mm^3) were fixed whole in 10% formalin, whereas larger tumors were sectioned longitudinally into two or three portions, one of which was fixed in 10% formalin, stained with hematoxylin and eosin and analyzed by light microscopy. Other portions were stored at −80°C for molecular analyses. After tumors were removed, colons from rats treated with BrdU were fixed in 10% buffered formalin and embedded longitudinally in paraffin, from which serial sections were cut for immunostaining.

Immunostaining used the BrdU *in situ* detection kit (BD Bioscience, San Diego, CA) according to the manufacturer's instructions. Sections were dewaxed and rehydrated, and after antigen retrieval with BD™ Retrieval A working solution in a microwave oven (80°C, 10 min) and slow cooling >20 min, slides were blocked for 10 min with 3% H_2O_2, rinsed three times in PBS and incubated with biotinylated anti-BrdU monoclonal antibody (1:40 dilution) for 1 h in a humidified chamber. After reaction with streptavidin peroxidase, sections were stained with Nova Red (Vector Laboratories, Burlingame, CA) and counterstained with hematoxylin.

Cleaved caspase-3 was determined using the EnVision+System–HRP Kit (Dako, Carpinteria, CA). Sections were dewaxed, rehydrated, rinsed with Dako AR buffer and then heated in a pressure cooker (121°C) for 5 min, followed by 20 min cooling at room temperature. After washing with water, endogenous peroxidases were blocked by incubating sections in 3% H_2O_2 in Dako TBST for 10 min, followed by Tris-buffered saline Tween-20 solution (TBST) alone. Sections were blocked with Dako serum-free protein for 10 min and then covered with polyclonal rabbit anticleaved caspase-3 (1:50 dilution in PBS), which specifically detects the endogenous large fragment of cleaved caspase-3 resulting from cleavage adjacent to Asp175 (Cell Signaling Technology, Danvers, MA). Sections were developed with Nova Red for 7 min, rinsed in water and counterstained with hematoxylin.

Labeling indices were determined based on the number of positive cells/total cells per crypt, using at least 45 well-distinguished crypts per rat; that is at least 15 crypts in the distal, middle and proximal regions of the colon. Only complete, well-oriented, longitudinally sectioned crypts with lumen at the top and muscularis mucosae at the base were evaluated.

Immunoblotting

Western analyses of β-catenin and c-Myc, normalized to β-actin, were examined as described before (3,4). In brief, frozen samples of tumors and adjacent normal-looking tissue were thawed and homogenized in lysis buffer, then centrifuged at 15 000 r.p.m. for 5 min and the supernatant (20 μg protein) was separated by sodium dodecyl sulfate–polyacrylamide gel electrophoresis on a 4–12% bis–Tris gel (Novex, Invitrogen, Carlsbad, CA), followed by transfer to nitrocellulose membrane (Invitrogen). Equal protein loading was confirmed by Amido Black staining. The membrane was blocked for 1 h with 2% bovine serum albumin, followed by incubation with primary antibody overnight at 4°C, ending with secondary antibody conjugated with horseradish peroxidase (Bio-Rad, Hercules, CA). Primary antibodies were as reported (3).

Quantitative real-time polymerase chain reaction

Isolation of messenger RNA (mRNA) from tissues and quantification of β-catenin gene (*Ctnnb1*) (rat), *cyclin D1*, *c-myc*, *c-jun* and *glyceraldehyde-3-phosphate dehydrogenase* were performed using the methodology reported by Wang *et al.* (13).

Single-strand conformation polymorphism and direct sequencing

Screening for β-catenin mutations by polymerase chain reaction (PCR)-based single-strand conformation polymorphism analysis coupled with direct sequencing was performed using the methodology reported elsewhere (3,4,13).

Statistics

Tumor incidence and multiplicity (number of tumors/tumor-bearing animal) were compared by logistic regression and non-parametric rank tests, respectively. Student's *t*-test and analysis of variance were used, respectively, for pairwise and group comparisons of molecular data.

Results

Survival was enhanced by EGCG but reduced by caffeine

The concentrations of EGCG and caffeine used here were similar to those present in brewed white tea beverage and did not adversely affect body weights for the first few weeks after the start of their administration; indeed, a slight gain in body weights was detected for the three treatment groups versus the control group, but this was not statistically significant (data not presented). Some of the animals were euthanized early due to the presence of large Zymbal's gland or skin tumors, whereas others suddenly lost appetite and/or body weight and at necropsy presented with colon or other tumors. In the PhIP/HF control group, the first sign of morbidity appeared at day 154, and less than one-third of the animals (32%) survived to the end of 1 year (Figure 1). In the group post-treated with EGCG, the first sign of morbidity was delayed significantly, until day 243, and the overall survival rate at 1 year was 49% ($P = 0.033$ versus PhIP/HF controls, Wilcoxon test). In the group post-treated with caffeine, initial signs of morbidity were seen as early as day 128, and only 18% survived to 1 year ($P = 0.013$ versus PhIP/HF controls). In rats post-treated with white tea, the first sign of morbidity was on day 132, fully 3 weeks before PhIP/HF controls showed morbidity, but 52% survived to 1 year; there was no significant difference overall compared with PhIP/HF controls ($P = 0.580$, trend analysis).

Unexpected promotion of colon tumors by white tea and caffeine

No tumors were detected in any of the vehicle/HF groups when the study was terminated after 1 year, but a broad spectrum of tumors was seen in animals given PhIP/HF diet (Table I). As expected, the colon was the most common target organ, and 41.6% of the PhIP/HF controls developed adenocarcinomas of the colon (Table I). In the same group, the incidence of tumors at other sites after 1 year was as follows: skin 27.8%, small intestine adenocarcinomas 19.4%, Zymbal's gland sebaceous squamous cell carcinomas 11.1%, acinary pancreatic adenocarcinomas 5.6% and salivary gland adenocarcinomas 5.6%. A similar range of tumors was reported before in rats given PhIP, including

Table I. Cumulative incidence of colon and non-colon tumors induced in the rat by three short cycles of PhIP/HF diet, and the effects of EGCG, white tea and caffeine given post-initiation

Tumor site/target organ	PhIP/HF controls (%)	PhIP/HF + EGCG (%)	PhIP/HF + white tea (%)	PhIP/HF + caffeine (%)
Colon (primary target organ)	41.6	43.6	68.5*	73.3*
Non-colon (other tumor sites)				
Skin	27.8	23.1	21.9	6.7
Small intestine	19.4	7.7	12.5	6.7
Zymbal's gland	11.1	7.7	3.1	0
Pancreas	5.6	0	3.1	0
Salivary gland	5.6	0	3.1	0
Bladder	0	2.6	3.1	0
Mammary gland	0	0	3.1	0
All non-colon combined[a]	69.5	48.7	46.9	13.3***

The data shown in the table are cumulative and include animals that were euthanized early before the study was finally terminated at 1 year.
[a]Includes other occasional rare tumors—sarcoma, lymphoma, osteosarcoma and fibrous histocytoma.
*$P < 0.05$, ***$P < 0.001$ versus PhIP/HF controls.

pancreatic tumors (14), although to our knowledge this is the first observation of PhIP-induced salivary gland tumors. Histopathology studies identified a wide spectrum of lesions in the skin, including sebaceous adenoma, sebaceous epithelioma, squamous cell carcinoma, papilloma, keratoacanthoma, cystic basal cell tumor and basal cell carcinoma. PhIP was reported as a prostate carcinogen when fed continuously in the diet for 1 year (15), but no prostate lesions were detected in the present investigation or in a prior study that cycled PhIP/HF (7).

In contrast to our previous findings on PhIP-induced ACF (12), no protective effects were seen for EGCG against the development of colon tumors at 1 year (43.6% final incidence, Table I). Moreover, in rats post-treated with white tea and caffeine, the colon tumor incidence was increased significantly to 68.5 and 73.3%, respectively, compared with 41.6% in the PhIP/HF controls ($P = 0.025$ and 0.039, using the Pearson's chi-square test). Interestingly, however, caffeine posttreatment reduced the tumor incidence in several other target organs; for all non-colon tumors combined, the final cumulative incidence was 13.3% (Table I) compared with 69.5% in the PhIP/HF controls ($P = 0.0003$). The corresponding incidence data for EGCG (48.7%) and white tea (46.9%) were not statistically different from the controls for all non-colon tumors combined.

In addition to the increase in colon tumor incidence, white tea and caffeine (but not EGCG) also increased the colon tumor volume ($P = 0.012$ and 0.009, respectively, versus controls, Figure 2). No significant differences were seen for tumor multiplicity, but the trends were similar; the corresponding data were as follows (colon tumors/colon tumor-bearing animal, mean ± standard error): PhIP/HF controls 1.47 ± 0.19, PhIP/HF + EGCG 1.27 ± 0.14, PhIP/HF + white tea 1.91 ± 1.15 and PhIP/HF + caffeine 2.18 ± 0.50 ($P > 0.05$, for all group comparisons, Wilcoxon test).

Altered frequency and spectrum of β-catenin mutations

We next examined β-catenin mutations in colon tumors using PCR-based single-strand conformation polymorphism analysis followed by direct sequencing. The frequency of β-catenin mutations was similar for controls and groups given EGCG or white tea, but significantly higher in rats post-treated with caffeine (Figure 3A). Specifically, in PhIP/HF controls, 36% (5/14) of the colon tumors harbored β-catenin mutations compared with 79% (11/14) after caffeine posttreatment ($P = 0.022$, Pearson's chi-square test). Although slightly elevated at 47.1% (8/17) and 40% (10/25) in the colon tumors from the rats post-treated with EGCG and white tea, respectively, these mutation frequencies were not significantly different from controls.

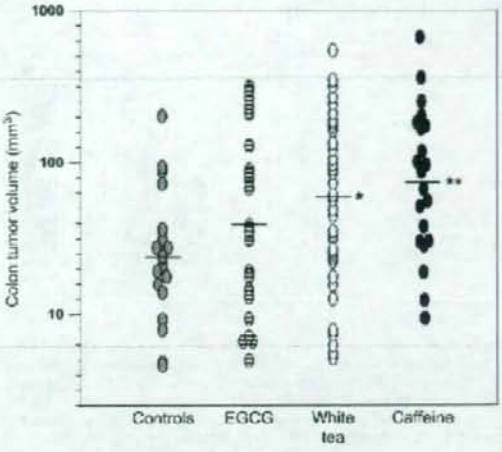

Fig. 2. White tea and caffeine increase colon tumor volume in the rat. Each data point represents a single colon tumor induced by PhIP/HF treatment (see Figure 1A for the dosing protocol). *$P < 0.05$ and **$P < 0.01$ compared with controls. Note that the data include colon tumors from animals that were euthanized early before the study was terminated at 1 year.

In addition to the increase in β-catenin mutation frequency, caffeine also produced a shift in the β-catenin mutation spectrum (Figure 3B). Thus, whereas β-catenin mutations were distributed more or less equally between codons 32 and 34 in controls and in groups given EGCG or white tea, in the colon tumors from rats post-treated with caffeine all but one of the mutations was detected in codon 34, and none were seen in codon 32 (black symbols, Figure 3B). Statistical analyses revealed that caffeine altered the spectrum of β-catenin mutations significantly compared with controls ($P = 0.017$, Fisher's exact test). Codons 32 and 34 represent 'hot spots' in *Ctnnb1* (4) and the corresponding mutations substitute Asp32 and Gly34, which flank Ser33, a key site for phosphorylation/ubiquitination in human and rat β-catenin (1,2).

β-Catenin and its downstream targets—role of c-myc in tumors promoted by tea and caffeine

Immunoblots revealed that β-catenin and c-Myc were more highly expressed in PhIP-induced colon tumors than in adjacent normal-looking tissue (Figure 4A). In addition, mRNA levels of *Ctnnb1*, *c-myc*, *c-jun* and *cyclin D1* were highly overexpressed in colon tumors compared with adjacent normal-looking tissue and in adjacent normal-looking tissue compared with normal colonic mucosa from untreated rats ($P < 0.001$ using Student's *t*-test, see pairwise comparisons indicated in Figure 4B).

The quantitative real-time PCR data were analyzed further, and we observed that colon tumors from rats given white tea or caffeine, but not EGCG, had significantly higher mRNA expression levels of *c-myc* ($P < 0.01$ versus controls, Figure 4C). No such association was seen for *Ctnnb1*, *c-jun* or *cyclin D1* and the posttreatment regimen (data not shown). When plotted as function of the β-catenin mutation status (Figure 4D), mRNA levels of *c-myc* were more highly expressed in colon tumors harboring codon 34 mutations than in tumors with wild-type β-catenin ($P < 0.01$) or codon 32 mutations ($P < 0.05$), and *Ctnnb1* mRNA expression also was higher in tumors with codon 34 mutations than wild-type β-catenin ($P < 0.01$).

Enhanced cell proliferation and reduced apoptosis during colon tumor promotion by white tea and caffeine

Immunostaining for BrdU incorporation revealed an expansion of the colonic crypt zone of cell proliferation in groups post-treated with

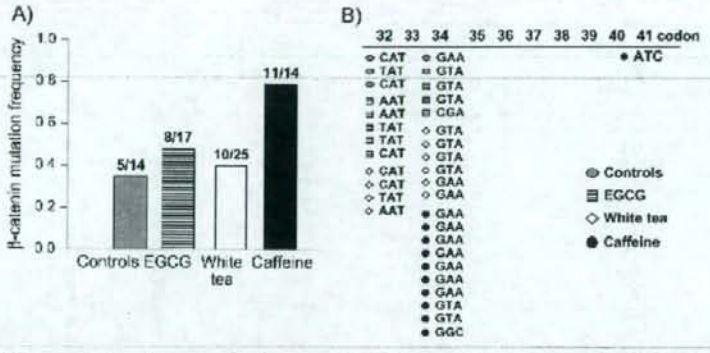

Fig. 3. Altered frequency and spectrum of β-catenin mutations in colon tumors. (**A**) β-Catenin mutations were screened by PCR-based single-strand conformation polymorphism analysis and direct sequencing, as before (3,4,13). Incidence data show the number of confirmed mutations/total samples analyzed by single-strand conformation polymorphism, above each corresponding bar. (**B**) Mutations were localized almost exclusively to codons 32 and 34 of the *Ctnnb1*, except for a codon 41 mutation in the caffeine group, which also completely lacked the codon 32 mutants detected in other groups. Data shown in the figure include colon tumors from animals that were euthanized before the study was terminated at 1 year.

caffeine and white tea, but not EGCG. The BrdU-labeling index, determined for the entire crypt column, was 12.1 ± 1.1% and 13.3 ± 0.5% in rats post-treated with white tea and caffeine, respectively, and augmented significantly versus 9.7 ± 0.9% in the PhIP/HF controls ($P < 0.05$, Figure 5A). The corresponding index for cleaved caspase-3, a measure of apoptosis, was 1.11 ± 0.38% and 0.68 ± 0.19% in rats post-treated with white tea and caffeine, respectively, which was significantly <2.44 ± 0.43% in the controls ($P < 0.05$ and $P < 0.01$, respectively, Figure 5B). Upon closer inspection, apoptotic cells were located mainly in the extreme apical crypt region for controls, but further down the crypt in rats post-treated with caffeine (Figure 5B). Cell proliferation and apoptosis indices were unaffected by posttreatment with EGCG. It is noteworthy that in rats given vehicle (no PhIP) and post-treated with white tea or caffeine, but not EGCG, the apoptosis index also was attenuated significantly versus the corresponding controls (data not presented).

Discussion

Ubagai *et al.* (7) described a protocol for the efficient induction of large intestine tumors in the rat by intermittent administration of PhIP and a HF diet. Specifically, 2 weeks of PhIP treatment at 400 p.p.m. in the diet were followed by 4 weeks of HF diet, which was repeated three times, ending with continuous feeding of HF diet for 42 weeks—this regimen produced a final incidence of large intestine tumors similar to that seen with continuous dietary PhIP treatment for an entire year (7). Although it reduced dramatically the amount of PhIP needed to produce colon tumors in the rat, we modified the protocol in order to further optimize carcinogen use. We also sought to eliminate HF exposure in the latter part of the study to facilitate post-initiation experiments with phytochemicals. Thus, PhIP was given by oral gavage at a dose (50 mg/kg body wt/day) that was matched to the daily carcinogen intake from 400 p.p.m. PhIP in the diet, and after three such cycles of PhIP/HF treatment, standard AIN-93M diet rather than HF diet was given until the study was terminated at 1 year. Using this modified protocol, the colon tumor incidence was 41.6%, comparable with the 45% incidence reported by Ubagai *et al.* (7). Animals in the PhIP/HF control group developed a wide spectrum of tumors (Table I) and less than one-third survived tumor free for 1 year (Figure 1). Rats were euthanized early due to the presence of Zymbal's gland tumors and/or skin lesions or after the appearance of blood in the stools, which was usually indicative of bleeding into the gastrointestinal tract from one or more tumors in the large or small intestine.

We reported previously (12) that white tea, EGCG and caffeine protected in the rat against PhIP-induced ACF, which are putative preneoplastic lesions and used as biomarkers of final colon tumor outcome (16–18). However, in the present investigation, EGCG had no inhibitory effect, and white tea and caffeine promoted rather than suppressed colon tumors. It is unclear whether this reflects a basic limitation of ACF as biomarkers of tumor outcome, as reported by others for genistein and cholic acid (19–21), or alternatively that caffeine and white tea exert a true biphasic response in the rat colon, being beneficial (protective) during short-term treatment but deleterious (promotional) after prolonged exposure. Importantly, however, we observed that caffeine offered significant protection in other target organs of PhIP-induced tumorigenesis (Table I). The cumulative results include animals that died early, but the overall trends were similar in each of the treatment groups for rats that survived to 1 year (data not shown). We interpret this as evidence that protection by caffeine in other target organs was real, and not due to fewer rats surviving to 1 year. Previously (22), caffeine was reported to protect against PhIP-induced mammary tumors in female rats but also promoted tumor formation in the colon.

Consistent with their tumor-promoting activities, caffeine and white tea altered colonic crypt homeostasis by enhancing cell proliferation versus apoptosis (Figure 5). Similar findings were obtained before in rats given chlorophyllin or indole-3-carbinol, and colon tumor promotion was associated with a shift in the β-catenin mutation spectrum (3,4). Thus, we rationalized that a likely mechanism for tumor promotion by white tea and caffeine might be via the dysregulation of β-catenin/Tcf signaling since β-catenin mutation and increased β-catenin expression are clearly associated with tumor progression (1). An increase in β-catenin mutations thus would be consistent with enhanced tumor growth by caffeine and white tea.

An increase in β-catenin mutation frequency coupled with a shift in the β-catenin mutation spectrum indeed was observed in colon tumors from rats post-treated with caffeine, but not white tea, indicating that β-catenin mutation status alone could not explain the promotional activities seen here. The colon tumors from rats given caffeine harbored codon 34 β-catenin mutants at a higher frequency than codon 32 mutants, suggesting that one or more promotional mechanisms 'selected' certain oncogenic forms of β-catenin to progress in preference to others. We do not know the reason for this apparent selection pressure, given that oncogenic β-catenin mutants with substitutions at either Asp32 or Gly34 were equally effective in activating a β-catenin/Tcf-responsive reporter construct (3,23).

Downstream targets of β-catenin/Tcf were highly expressed in colon tumors, namely *c-myc*, *c-jun* and *cyclin D1* and so too was *Ctnnb1* mRNA itself. Overexpression of β-catenin protein therefore might arise due to mutational events that stabilize the β-catenin protein

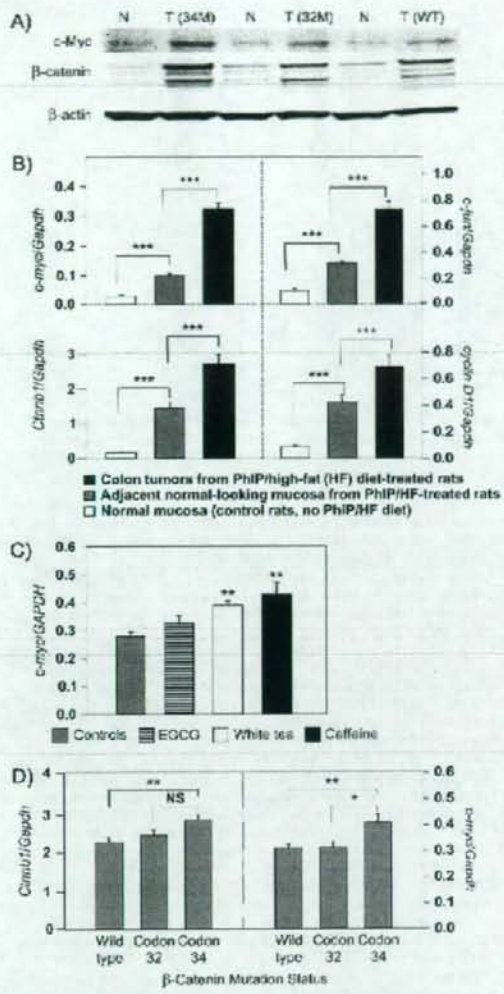

Fig. 4. Overexpression of β-catenin and β-catenin/Tcf target genes in rat colon tumors induced by PhIP/HF treatment. (**A**) Immunodetection of β-catenin and c-Myc in colon tumors (T) and adjacent normal-looking tissue (N). The loading control was β-actin. Blots shown are representative data from more than a dozen tumors, each with mutations in *Ctnnb1* codon 32 (32M), codon 34 (34M) or wild-type (WT), respectively. (**B**) Quantitative real-time PCR was used to examine *Ctnnb1*, *c-myc*, *c-jun* and *cyclin D1* mRNA levels, normalized to *glyceraldehyde-3-phosphate dehydrogenase* (*Gapdh*). Data = mean ± standard error, $^{***}P < 0.001$. (**C**) Quantitative real-time PCR data for *c-myc* (mean ± standard error) plotted as a function of posttreatment regimen; $^{**}P < 0.01$ versus controls. No significant differences were seen for the corresponding data on *c-jun*, *cyclin D1* or *Ctnnb1* (data not shown). (**D**) Quantitative real-time PCR data for *Ctnnb1* and *c-myc* (mean ± standard error) plotted as a function of β-catenin mutation status. $^{*}P < 0.05$, $^{**}P < 0.01$; NS, not significant. No significant changes were seen for corresponding data on *c-jun* and *cyclin D1* (data not shown). Data in the figure are cumulative and include colon tumors from animals that were euthanized before the study was terminated at 1 year.

(1) or via dysregulation of *Ctnnb1* expression at the transcriptional level, as reported for 1,2-dimethylhydrazine-induced colon tumors (13). Importantly, among the three β-catenin/Tcf target genes examined, only *c-myc* showed any concordance with tumor promotion by white tea and caffeine (Figure 4C). Thus, rather than β-catenin, c-Myc overexpression may be important in the promotional mechanism of white tea and caffeine. In its capacity as an ataxia telangiectasia mutated/ATM and Rad3-related kinase inhibitor, caffeine was reported to prevent p53 accumulation upon activation of c-Myc or E2F1 (24). We recently described a pathway in which overexpression of c-Myc elevated E2F1 and enhanced Bcl-2 levels, resulting in suppression of apoptosis (25). Suppression of apoptosis in the present study was evident for caffeine and white tea using cleaved caspase-3 as a biomarker, in animals treated with PhIP/HF diet and also in the negative controls given three cycles of vehicle/HF diet. However, we did not examine the possible role of E2F1, Bcl-2 or p53 in the promotional mechanism of caffeine and white tea in the rat colon, and this is worthy of future study.

Finally, it is important to note that a substantial literature exists on tea and coffee consumption in humans, which does not indicate an adverse effect on tumor outcome—indeed, some studies suggest a protective role for these caffeinated beverages. For example, Tavani *et al.* (26) reviewed epidemiological studies for the period 1990–2003 on coffee, decaffeinated coffee and tea and cancer of the colon and rectum. For coffee consumption, most case–control studies found risk estimates below unity for colon cancer, but no relation for rectal cancer. A meta-analysis of 5 cohort and 12 case–control studies found a pooled relative risk of 0.75 for colon cancer, which was significant. No such relationship was seen for tea or decaffeinated coffee. A more recent meta-analysis (27) concluded that 'despite the strong evidence from *in vitro* and non-human *in vivo* studies in support of green and black tea as potential chemopreventive agents against colorectal cancer, available epidemiologic data are insufficient to conclude that either tea type may protect against colorectal cancer in humans'. In light of the findings from the present investigation and the increased risk for colorectal adenoma associated with meat cooked at high temperature (28), it would be interesting to reassess the epidemiological evidence for possible increased risk of colon cancer in a subset of individuals consuming tea (or coffee) plus large amounts of cooked meat and a HF diet.

In summary, we report here that in rats treated with three short cycles of PhIP/HF diet, post-initiation exposure to white tea and caffeine promoted rather than suppressed colon tumorigenesis, whereas EGCG had no effect. Caffeine increased the frequency of β-catenin mutations, and the colon tumors harbored almost exclusively β-catenin mutants with direct substitutions of Gly34. One important conclusion from these studies is that the final spectrum of β-catenin mutants in colon tumors is clearly influenced by exposure to dietary phytochemicals, as reported before for chlorophyllin and indole-3-carbinol (3,4). There was no direct concordance between the changes in tumor outcome and the expression of β-catenin or its downstream target genes. However, c-Myc was identified as a possible key player in the promotional mechanism of white tea and caffeine. Caffeine protected in other target organs of PhIP-induced tumorigenesis, suggesting a complex pattern of tumor modulation, in line with the general heterogeneity noted in human epidemiology studies of caffeinated beverages.

Supplementary material

The colour version of figure 5 can be found at http://carcin.oxfordjournals.org/

Funding

Inko's White Tea (New York, NY) and National Institutes of Health (CA90890, CA65525 and CA122959); Foundation for Promotion of Cancer Research, Tokyo, Japan to R.H.D.

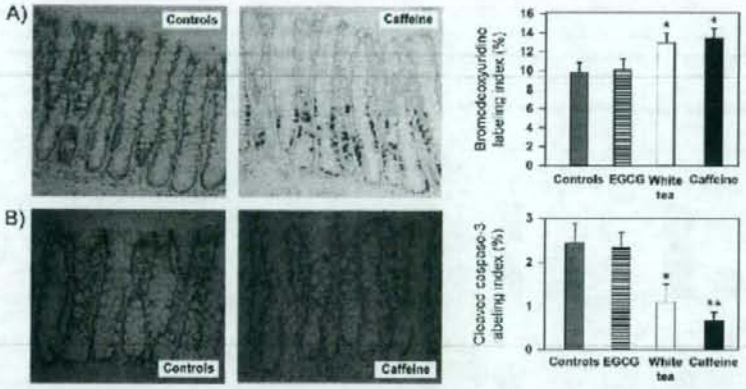

Fig. 5. Cell proliferation and apoptosis in rat colonic mucosa after posttreatment with white tea, EGCG and caffeine. Immunodetection of (**A**) bromodeoxyuridine incorporation and (**B**) cleaved caspase-3, and the corresponding labeling indices determined for the entire colonic crypt. The number of positively stained cells was divided by the total number of cells and multiplied by 100 to obtain 'percent labeling' for the entire crypt. Data = mean ± standard error, $^{*}P < 0.05$, $^{**}P < 0.01$ versus controls (Note: color versions of these images are avaliable as supplementary data on the *Carcinogenesis* website).

Acknowledgements

We thank Barbara Delage, Qingjie Li, Tianwei Yu, Gayle Orner, Valerie Elias, Kate Cleveland and Christine Larsen for assistance with necropsy examinations. Laboratory Animal Service staff are gratefully acknowledged for their help with animal care and maintenance. C.Riegger of DSM Nutritional Products kindly provided the EGCG (TEAVIGO™). Mutan White tea was a generous gift from Stash Tea Co.

Conflict of Interest Statement: None declared.

References

1. Schneikert,J. *et al.* (2007) The canonical Wnt signalling pathway and its APC partner in colon cancer development. *Gut*, **56**, 417–425.
2. Al-Fageeh,M. *et al.* (2004) Phosphorylation and ubiquitination of oncogenic mutants of beta-catenin containing substitutions at Asp32. *Oncogene*, **23**, 4839–4846.
3. Blum,C.A. *et al.* (2001) Beta-Catenin mutation in rat colon tumors initiated by 1,2-dimethylhydrazine and 2-amino-3-methylimidazo[4,5-*f*]quinoline, and the effects of post-initiation treatment with chlorophyllin and indole-3-carbinol. *Carcinogenesis*, **22**, 315–320.
4. Blum,C.A. *et al.* (2003) Mutational analysis of *Ctnnb1* and *Apc* in tumors from rats given 1,2-dimethylhydrazine and 2-amino-3-methylimidazo[4,5-*f*]-quinoline: mutational 'hotspots' and the relative expression of beta-catenin and c-jun. *Mol. Carcinog.*, **36**, 195–203.
5. Sugimura,T. *et al.* (2004) Heterocyclic amines: mutagens/carcinogens produced during cooking of meat and fish. *Cancer Sci.*, **95**, 290–299.
6. Dashwood,R.H. *et al.* (1998) High frequency of beta-catenin (*Ctnnb1*) mutations in the colon tumors induced by two heterocyclic amines in the F344 rat. *Cancer Res.*, **58**, 1127–1129.
7. Ubagai,T. *et al.* (2002) Efficient induction of rat large intestinal tumors with a new spectrum of mutations by intermittent administration of 2-amino-1-methyl-6-phenylimidazo[4,5-*b*]pyridine in combination with a high fat diet. *Carcinogenesis*, **23**, 197–200.
8. Santana-Rios,G. *et al.* (2001) Potent antimutagenic activity of white tea in comparison with green tea in the Salmonella assay. *Mutat. Res.*, **495**, 61–74.
9. Dashwood,W.M. *et al.* (2002) Inhibition of β-catenin/Tcf activity by white tea, green tea, and epigallocatechin-3-gallate (EGCG): minor contribution of H_2O_2 at physiologically relevant EGCG concentrations. *Biochem. Biophys. Res. Commun.*, **296**, 584–588.
10. Orner,G.A. *et al.* (2003) Suppression of tumorigenesis in the Apc^{min} mouse: down-regulation of β-catenin signaling by a combination of tea plus sulindac. *Carcinogenesis*, **24**, 263–267.
11. Santana-Rios,G. *et al.* (2001) Inhibition by white tea of 2-amino-1-methyl-6-phenylimidazo[4,5-*b*]pyridine-induced colonic aberrant crypts in the F344 rat. *Nutr. Cancer*, **41**, 98–103.
12. Carter,O. *et al.* (2007) Comparison of white tea, green tea, epigallocatechin-3-gallate and caffeine as inhibitors of PhIP-induced colonic aberrant crypts in the rat. *Nutr. Cancer*, **58**, 60–65.
13. Wang,R. *et al.* (2006) Tumors from rats given 1,2-dimethylhydrazine plus chlorophyllin or indole-3-carbinol contain transcription changes in β-catenin that are independent of the β-catenin mutation status. *Mutat. Res.*, **601**, 11–18.
14. Ogawa,K. *et al.* (1998) Modification by 2-amino-1-methyl-6-phenylimidazo[4,5-*b*]pyridine (PhIP) of 3,2'-dimethyl-4-aminobiphenyl (DMAB)- induced rat pancreatic and intestinal tumorigenesis. *Cancer Lett.*, **124**, 31–37.
15. Shirai,T. *et al.* (1997) The prostate: a target organ for carcinogenicity of 2-amino-1-methyl-6-phenylimidazo[4,5-*b*]pyridine (PhIP) derived from cooked foods. *Cancer Res.*, **57**, 195–198.
16. Bird,R.P. *et al.* (2000) The significance of aberrant crypt foci for understanding the pathogenesis of colon cancer. *Toxicol. Lett.*, **112–113**, 395–402.
17. Stevens,R.G. *et al.* (2007) Epidemiology of colonic aberrant crypt foci: review and analysis of existing studies. *Cancer Lett.*, **252**, 171–183.
18. Corpet,D.E. *et al.* (2002) Most effective colon cancer chemopreventive agents in rats: a systematic review of aberrant crypt foci and tumor data, ranked by potency. *Nutr. Cancer*, **43**, 1–21.
19. Pereira,M.A. *et al.* (1994) Use of azoxymethane-induced foci of aberrant crypts in rat colon to identify potential cancer chemopreventive agents. *Carcinogenesis*, **15**, 1049–1054.
20. Rao,C.V. *et al.* (1997) Enhancement of experimental colon cancer by genistein. *Cancer Res.*, **57**, 3717–3722.
21. Shirtliff,N. *et al.* (1996) Growth features of aberrant crypt foci that resist modulation by cholic acid. *Carcinogenesis*, **17**, 2093–2096.
22. Hagiwara,A. *et al.* (1999) Organ- dependent modifying effects of caffeine, and two naturally occurring antioxidants alpha-tocopherol and n-tritriacontane-16,18-dione, on 2-amino-1-methyl-6-phenylimidazo[4,5-b]pyridine (PhIP)-induced mammary and colonic carcinogenesis in female F344 rats. *Jpn. J. Cancer Res.*, **90**, 399–405.
23. Porfiri,E. *et al.* (1997) Induction of a beta-catenin-LEF-1 complex by wnt-1 and transforming mutants of beta-catenin. *Oncogene*, **15**, 2833–2839.
24. Lindstrom,M.S. *et al.* (2003) Myc and E2F1 induce p53 through p14ARF-independent mechanisms in human fibroblasts. *Oncogene*, **22**, 4993–5005.
25. Li,Q. *et al.* (2007) Bcl-2 over-expression in PhIP-induced colon tumors: cloning of the rat *Bcl-2* promoter and characterization of a pathway involving β-catenin, c-Myc and E2F1. *Oncogene*, **26**, 6194–6202.
26. Tavani,A. *et al.* (2004) Coffee, decaffeinated coffee, tea and cancer of the colon and rectum: a review of epidemiological studies, 1999–2003. *Cancer Causes Control*, **15**, 743–757.
27. Sun,C.L. *et al.* (2006) Green tea, black tea and colorectal cancer risk: a meta-analysis of epidemiologic studies. *Carcinogenesis*, **27**, 1301–1309.
28. Sinha,R. *et al.* (2005) Meat, meat cooking methods and preservation, and risk of colorectal adenoma. *Cancer Res.*, **65**, 8034–8041.

Received January 16, 2008; revised February 4, 2008; accepted February 8, 2008

Mutation Research 673 (2009) 9–20

Contents lists available at ScienceDirect

Mutation Research/Genetic Toxicology and Environmental Mutagenesis

journal homepage: www.elsevier.com/locate/gentox
Community address: www.elsevier.com/locate/mutres

Dose-dependent alterations in gene expression in mouse liver induced by diethylnitrosamine and ethylnitrosourea and determined by quantitative real-time PCR☆

Takashi Watanabe[a], Gotaro Tanaka[b], Shuichi Hamada[c], Chiaki Namiki[d], Takayoshi Suzuki[e], Madoka Nakajima[f], Chie Furihata[a,*]

[a] Functional Genomics Laboratory, School of Science and Engineering, Aoyama Gakuin University, Fuchinobe 5-10-1, Sagamihara, Kanagawa 229-0006, Japan
[b] Tokushima Research Center, Taiho Pharmaceutical Co. Ltd., Hiraishiebisuno 224-2, Kawauchichou, Tokushima, Tokushima 771-0194, Japan
[c] Genetic Toxicology Group, Toxicology Division II, Kashima Laboratory, Mitsubishi Chemical Safety Institute Ltd., Sunayama 14, Kamisu-shi, Ibaraki 314-0255, Japan
[d] Central Research Laboratory, SSP Co. Ltd., Nanpeidai 1143, Narita, Chiba 286-8511, Japan
[e] Division of Cellular & Gene Therapy Products, National Institute of Health Sciences, Kamiyoga 1-18-1 Setagaya-ku, Tokyo 158-8501, Japan
[f] Genetic Toxicology Group, Biosafety Research Center, Foods, Drugs, and Pesticides, Shioshinden 582-2, Fukude-cho, Iwata-gun, Shizuoka 437-1213, Japan

ARTICLE INFO

Article history:
Received 29 September 2008
Received in revised form 31 October 2008
Accepted 9 November 2008
Available online 21 November 2008

Keywords:
Genotoxic carcinogens
Dose-dependent alteration
Hierarchical clustering
k-means clustering
IPA

ABSTRACT

We examined the dose-dependency of gene expression changes for 51 genes in mouse liver treated with two *N*-nitroso genotoxic hepatocarcinogens, diethylnitrosamine (DEN) and ethylnitrosourea (ENU) by quantitative real-time PCR (qPCR). DEN (3, 9, 27 and 80 mg/kg bw) or ENU (6, 17, 50 and 150 mg/kg bw) was injected intraperitoneally into groups of five male 9-week-old B6C3F$_1$ mice and the livers were dissected after 4 h and 28 days. Total RNA from pooled livers was reverse-transcribed to cDNA and the amount of each gene was quantified by qPCR. Results were analyzed by hierarchical and *k*-means clustering and ingenuity pathway analysis (IPA). The most characteristic result was a similar dose-dependency of gene expression changes with DEN and ENU. Twenty-one genes exhibited a distinct dose-dependent increase in expression at 4 h for both carcinogens [*Bax*, *Btg2*, *Ccng1*, *Cdkn1a*, *Cyp4a10*, *Cyp21a1*, *Fos*, *Gadd45b*, *Gdf15*, *Hmox1*, *Hspb1*, *Isg20l1*, *Jun*, *Mbd1*, *Mdm2*, *Myc*, *Net1*, *Plk2*, *Ppp1r3c*, *Rcan1* and *Tubb2c*], although the increase in gene expression due to ENU was generally weaker than that due to DEN. Only *Gdf15* showed a dose-dependent increase in expression at 28 days for both carcinogens. The differences between DEN and ENU were in the expression of additional genes (7 for DEN and 8 for ENU). IPA extracted five gene networks: Network-1 included genes related to cancer and cell cycle arrest and associated with *Bax*, *Btg2*, *Ccng1*, *Cdkn1a*, *Gadd45b*, *Gdf15*, *Hspb1*, *Mdm2* and *Plk2* and Network-2 was related to DNA replication, recombination, repair and cell death and associated with *Cyp21a1*, *Gdf15*, *Ppp1r3c*, *Rcan1* and *Tubb2c*. The present results show a distinct dose-dependency of gene expression changes induced by DEN and ENU. These changes were associated with cancer, cell cycle arrest, DNA replication, recombination, repair and cell death and were seen not only at 4 h but also, for some, at 28 days after administration.

1. Introduction

Diethylnitrosamine (DEN) and ethylnitrosourea (ENU) are potent genotoxic *N*-nitroso carcinogens that induce hepatocellular carcinomas in mouse liver [1,2]. It has been reported that after its metabolic biotransformation, DEN produces the promutagenic adducts O^6-ethylguanine (O^6-EtG) and O^4- and O^2-ethylthymine and that O^4-ethylthymine may be responsible for the initiation of hepatocellular carcinomas in rats [3]. ENU, which is a direct-ethylating agent, forms several major adducts upon reaction with DNA, of which O^6-EtG, O^4- and O^2-ethylthymine and N^3-ethylthymine have been implicated in mutagenic lesions [4]. Suzuki et al. have reported that mutagenic activity by DEN and ENU was clearly detected with the *lacZ* mutation assay in mouse liver at 7 days [5]. Mientjes et al. have reported that the O^6-EtG levels increased as early as 1.5 h after treatment, whereas at 3 days more than 90% of the lesions had been removed from the DNA in the livers of DEN- and ENU-treated mice, based on *lacZ* transgenic mice [6]. After this period, however, with the bulk of O^6-EtG removed, the induction of *lacZ* mutations was observed at 3 days and continued to increase for some weeks.

☆ This work was a JEMS/MMS/Toxicogenomics group collaborative study.

* Corresponding author at: Department of Chemistry and Biological Science, School of Science and Engineering, Aoyama Gakuin University, 5-10-1 Fuchinobe, Sagamihara, Kanagawa 229-8558, Japan. Tel.: +42 759 6233; fax: +42 759 6511.
E-mail address: chiefurihata@gmail.com (C. Furihata).

1383-5718/$ – see front matter © 2008 Elsevier B.V. All rights reserved.
doi:10.1016/j.mrgentox.2008.11.004

Previously, Waring et al. showed by DNA microarray that a number of genes are up-regulated and down-regulated in rat liver, with rats dosed daily with DEN for 3 days and euthanized on the 4th day [7]. Genes up-regulated by DEN included genes related to growth arrest and DNA damage, such as *Bax*, *Ccnd1*, *Ccng1*, *Cdkn1a/p21*, *Gadd45* and *Jun*. However, no studies have focused on either the DNA damaging time of 4 h or the mutation fixing time of 28 days in DEN-treated mouse or rat liver. Although it has been reported that ENU induced expression of *Bax*, *Crp*, *Cyp2a*, *Gstm2*, *Icam1*, *Mig*, and *Mt2* mRNA in mouse liver, little is known about differential gene expression in ENU-exposed rodent liver [8].

Quantitative real-time PCR (qPCR) is an alternative technology for toxicogenomics [9]. qPCR is a highly regarded and reliable quantitative method but analysis of a large number of genes may be lengthy. It is impractical to examine a great number of genes with qPCR. Therefore, we selected 51 candidate genes (Table 1) based on our previous results using the Affymetrix GeneChip Mu74AV2 and original DNA microarray to determined the effects of DEN, dimethylnitrosamine, dipropylnitrosamine, ENU, *o*-aminoazotoluene, 7,12-dimethylbenz[*a*]anthracene, dibenzo[*a*,*l*]pyrene, phenobarbital and ethanol exposure in mouse liver for 4 and 20 h and 14 and 28 days in our JEMS/MMS/Toxicogenomics group collaborative study; results were reported in part [10]. We examined gene expression changes at an early time after administration, as we were interested in whether toxicogenomics was useful for carcinogen screening. In the previous study, using a single dose for each chemical, gene expression changes in number and degree were observed to peak at 4 h after administration. It is known that genotoxic *N*-nitroso carcinogens induce DNA damage and repair in a matter of a few hours after their administration; DNA adducts [6], DNA strand-breaks [11], unscheduled DNA synthesis [12] and other lesions have been reported. It is also known that mutations are observed in transgenic mouse liver 28 days after genotoxic *N*-nitroso carcinogen administration [5,6]. However, related gene expression changes at these time points have not yet been fully elucidated.

Table 1
Fifty-one genes examined in the present study.

No.	Symbol	Gene name	Accession number
1	*Bax*	Bcl2-associated X protein	NM_007527
2	*Bcl2*	B-cell leukemia/lymphoma 2	NM_009741
3	*Btg2*	B-cell translocation gene 2, anti-proliferative	NM_007570
4	*Casp1*	IL-1B converting enzyme; interleukin 1 beta-converting enzyme	NM_009807
5	*Ccnf*	Cyclin F	NM_007634
6	*Ccng1*	Cyclin G1	NM_009831
7	*Ccng2*	Cyclin G2	NM_007635
8	*Cdkn1a (p21)*	Cyclin-dependent kinase inhibitor 1A (P21)	NM_007669
9	*Cyp1a1*	Cytochrome P450, family 1, subfamily a, polypeptide 1	NM_009992
10	*Cyp1a2*	Cytochrome P450, family 1, subfamily a, polypeptide 2	NM_009993
11	*Cyp4a10*	Cytochrome P450, family 4, subfamily a, polypeptide 10	NM_010011
12	*Cyp21a1*	Cytochrome P450, family 21, subfamily a, polypeptide 1	NM_009995
13	*Dpyd*	Dihydropyrimidine dehydrogenase	NM_170778
14	*Egfr*	Epidermal growth factor receptor	NM_207655
15	*Ephx1*	Epoxide hydrolase 1, microsomal	NM_010145
16	*Fabp5*	Fatty acid binding protein 5, epidermal	NM_010634
17	*Fos*	FBJ osteosarcoma oncogene	NM_010234
18	*Gadd45b*	Growth arrest and DNA-damage-inducible 45 beta	NM_008655
19	*Gadd45g*	Growth arrest and DNA-damage-inducible 45 gamma	NM_011817
20	*Gapdh*	Glyceraldehyde-3-phosphate dehydrogenase	NM_008084
21	*Gdf15*	Growth differentiation factor 15	NM_011819
22	*Glul*	Glutamate-ammonia ligase (glutamine synthetase)	NM_008131
23	*Gstk1*	Glutathione S-transferase kappa 1	NM_029555
24	*Gyk	Glycerol kinase	NM_212444
25	*Hist1h1c*	H1 histone family, member 2	NM_015786
26	*Hspa1b (Hsp70)*	Heat shock protein 1B	NM_010478
27	*Hspb1*	Heat shock protein 1	NM_013560
28	*Hspb2 (Hsp27)*	Heat shock protein 2	NM_024441
29	*Hmox1*	Heme oxygenase (decycling) 1	NM_010442
30	*Hprt1*	Hypoxanthine guanine phosphoribosyl transferase 1	NM_013556
31	*Igfbp1*	Insulin-like growth factor binding protein 1	NM_008341
32	*Isg20l1*	Interferon stimulated exonuclease gene 20-like 1	NM_026531
33	*Jun*	Jun oncogene	NM_010591
34	*Kras*	v-Ki-ras2 Kirsten rat sarcoma viral oncogene homolog	NM_021284
35	*Lig3*	Ligase III, DNA, ATP-dependent	NM_010716
36	*Lrp1*	Low density lipoprotein receptor-related protein 1	NM_008512
37	*Mbd1*	Methyl-CpG binding domain protein 1	NM_013594
38	*Mdm2*	Transformed mouse 3T3 cell double minute 2	NM_010786
39	*Myc*	Myelocytomatosis oncogene	NM_010849
40	*Net1*	Neuroepithelial cell transforming gene 1	NM_019671
41	*Pdgfb*	Platelet-derived growth factor, B polypeptide	NM_011057
42	*Plk2*	Polo-like kinase 2; serum-inducible kinase	NM_152804
43	*Pml*	Promyelocytic leukemia	NM_008884
44	*Pmm1*	Phosphomannomutase 1	NM_013872
45	*Ppp1r3c*	Protein phosphatase 1, regulatory (inhibitor) subunit 3C	NM_016854
46	*Rad52*	RAD52 homolog (S. cerevisiae)	NM_011236
47	*Rcan1(Dscr1)*	Regulator of calcineurin 1	NM_019466
48	*Trp53*	Transformation related protein 53	NM_011640
49	*Tubb2c*	Tubulin, beta 2c	NM_146116
50	*Ube2e1 (UbcM3)*	Ubiquitin-conjugating enzyme E2E 1, UBC4/5 homolog (yeast)	NM_009455
51	*Ung*	Uracil-DNA glycosylase	NM_011677

In this paper, we report our studies of gene expression changes in B6C3F$_1$ mouse liver induced by multiple doses of two typical alkylating agents, DEN and ENU. We investigated the dose-dependency of gene expression changes at two different time points: 4 h, characterized by the production of many DNA lesions, and 28 days, characterized by fixing of mutations [6]. If we could show dose-dependency in gene expression changes at 4 h, we could clarify key genes related to DNA lesions and subsequent various phenomena in liver cells induced by DEN and ENU. If we could show the dose-dependency in gene expression changes at 28 days, we could clarify key genes related to effects of mutations and subsequent changes that may be causal for carcinogenesis. Our purpose is to determine biological cell responses induced by DEN and ENU by examining the dose-dependency at these two time points.

In addition, we examined gene networks using IPA to elucidate interactions between genes with altered expression.

2. Materials and methods

2.1. Animal treatment

Male B6C3F$_1$ mice were obtained at 8 weeks of age from Charles River Japan, Inc. (Yokohama, Japan). They were kept in plastic cages on wood chips as bedding and given food (Oriental MF, Oriental Yeast Co., Tokyo) and water *ad libitum* in an air-conditioned room [12 h light (7 a.m. to 7 p.m.), 12 h dark; 23 ± 2 °C; 55 ± 5% humidity]. All animal experiments were conducted in accordance with the NIH Guide for Care and Use of Laboratory Animals and approved by the Animal Care and Use Committee at the Mitsubishi Chemical Safety Institute Ltd.

Mice at 9 weeks of age were injected intraperitoneally (i.p.) with DEN (3, 9, 27 and 80 mg/kg bw; Wako Pure Chem. Ind. Ltd., Osaka, Japan; CAS 55-18-5) dissolved in sterile water or ENU (6, 17, 50 and 150 mg/kg bw; Wako Pure Chem. Ind. Ltd., Osaka, Japan; CAS 759-73-9) dissolved in sterile water. Control animals for the DEN- and ENU-treated groups received sterile water. At 4 h and 28 days after treatment, animals were sacrificed after which the liver was collected, frozen on dry ice, and stored at −80 °C until use.

2.2. RNA isolation and relative quantification by real-time PCR

To isolate total RNA, approximately 150 mg from each liver (main lobe) was placed into TRIzol reagent (Invitrogen Corp., Carlsbad, CA, USA) and immediately homogenized using a Potter homogenizer. The samples were further homogenized with a 1 ml syringe and 18 gauge needle. Finally, total RNA was purified using an ethanol precipitation method. Complementary DNA (cDNA) was yielded from total RNA using the SuperScript First strand synthesis system for RT-PCR kit (Invitrogen Corp.).

qPCR amplifications were performed in triplicate using the SYBR Green I assay in an Opticon II (MJ Research, Inc., Waltham, MA, USA). The reactions were carried out in a 96-well plate in 20-μl reactions containing 2× SYBR Green Master Mix (Applied Biosystems, Lincoln Centre Drive Foster City, CA, USA), 2 pmol each of forward and reverse primer, and a cDNA template corresponding to 10 ng total RNA. Each primer sequence and Ct value are shown in Table 2. We selected 51 genes based on our previous results from the original DNA microarray and Affymetrix GeneChip Mu74AV2 for samples after treatment of DEN, dimethylnitrosamine, dipropylnitrosamine, ENU, *o*-aminoazotoluene, 7,12-dimethylbenz[*a*]anthracene, dibenzo[*a*,*l*]pyrene, phenobarbital and ethanol in our JEMS/MMS/Toxicogenomics group collaborative study. *Gapdh* and *Hprt1* were selected as housekeeping genes. SYBR Green PCR conditions were 95 °C for 10 min, followed by 95 °C for 10 s, 58 °C for 50 s and 72 °C for 20 s, for 45 cycles. In each assay a standard curve was determined concurrently with examined samples. In the preliminary experiment the highest group was selected for each gene and was used as the standard sample in the subsequent assay. In each standard curve determination, there were six dilution series of standard samples, diluted up to 1/5, 1/25, 1/125, 1/625 and 1/3125 of the selected standard liver cDNA for each gene. Finally, relative quantitative values of each sample were determined with 1/25 diluted cDNA and were normalized with those of the *Gapdh* genes. Relative *Gapdh* expression levels of experimental groups are presented in Fig. 1.

2.3. Data analysis and clustering algorithm

For the cluster analysis program, we performed a logarithmic ($\log_2$) transformation of the data to stabilize the variance and the gene expression profile of each DEN- and ENU-treated sample, normalized to the median gene expression level for the entire sample set. Both hierarchical and *k*-means clustering were performed using GENESIS software (http://genome.tugraz.at/) [13] for each data set at 4 h and 28 days separately. Gene groups were presented automatically by hierarchical clustering. Four clusters were set up initially in *k*-means clustering based on hierarchical clustering results. Genes which belonged to dose–response groups by both clustering methods were defined as dose–response genes. Furthermore, genes which showed less than a 0.5-fold decrease dose-dependently were evaluated as decrease genes by expression pattern because the decrease genes were few and could not be extracted using both clustering methods.

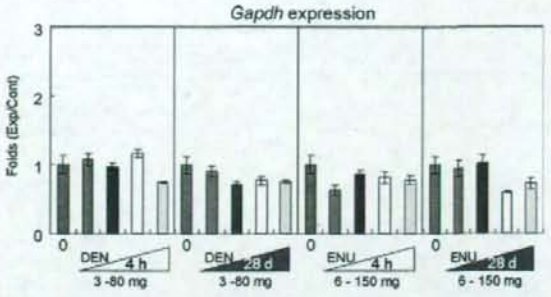

Fig. 1. Relative expression of *Gapdh*. DEN (0–80 mg/kg bw) and ENU (0–150 mg/kg bw) were given to 9-week-old mice (five per group). Total RNA was extracted from pooled liver and reverse-transcribed to cDNA. *Gapdh* expression was determined by qPCR in triplicate assays. Results are shown as mean ± S.D.

The color displays given in Fig. 2 show the $\log_2$ (expression ratio) as (1) red when the treatment sample is up-regulated relative to the control sample, (2) blue when the treatment sample is down-regulated relative to the control sample and (3) white when the $\log_2$ (expression ratio) is close to zero.

2.4. Pathway analysis

Numerical experimental data at 4 h and 28 days after DEN or ENU treatment were separately analyzed by ingenuity pathway analysis (IPA) Software-Complete Pathways Database. These data were generated through the use of IPA, a web-delivered application (www.Ingenuity.com) that enables the visualization and analysis of biologically relevant networks to discover, visualize, and explore therapeutically relevant networks. IPA information was extracted by experts from the full text of the scientific literature, including information about genes, drugs, chemicals, cellular and disease processes, and signaling and metabolic pathways.

Expression data sets containing gene identifiers (Entrez gene identifiers) and their corresponding expression values as fold changes were uploaded as a tab-delimited text file. Each gene identifier was mapped to its corresponding gene object in the Ingenuity Pathways Knowledge Base. To start building networks, the application program queries the Ingenuity Pathways Knowledge Base for interactions between focus genes and all other gene objects stored in the knowledge base and generates a set of networks. The program then computes a score for each network according to the fit of the network to the set of focus genes. The score indicates the likelihood of the focus genes in a given network being found together due to random chance. A score of >2 indicates that there is a <1 in 100 chance that the focus genes were assembled randomly into a network due to random chance.

3. Results

3.1. Dose-dependent alteration of gene expression induced by DEN

3.1.1. Clustering analysis for gene expression

Unsupervised hierarchical clustering results are shown in Fig. 2. The changes in gene expression are represented colorimetrically as described in Section 2. The clustering presented four groups (DEN-4 h-Grp-1 to DEN-4 h-Grp-4) and an ungrouped gene 4 h after administration, and three groups (DEN-28 d-Grp-1 to DEN-28 d-Grp-3) and eight ungrouped genes 28 days after administration. As unsupervised hierarchical clustering was performed for 4 h and 28-day samples separately, group member genes were different for 4 h groups and 28-day groups.

At 4 h, all 20 DEN-4 h-Grp-1 genes showed a dose-dependent increase of more than 3–64-fold. Twelve DEN-4 h-Grp-2 genes were suggested to have a gradual dose-dependent increase of less than that for the expression in DEN-4 h-Grp-1. Two DEN-4 h-Grp-4 genes exhibited a dose-dependent decrease of less than 0.3-fold.

Table 2
Primer sequences of 51 genes examined in the study.

No.	Symbol	Left	Right	Ct
1	*Bax*	CCAGGATGCGTCCACCAAGAAG	GGAGTCCGTGTCCACGTCAGC	28
2	*Bcl2*	GATGACTTCTCTCGTCGCTACC	CATCCCTGAAGAGTTCCTCCAC	31
3	*Btg2*	ACGGGAAGAGAACCGACATGC	ATGATCGGTCAGTGCGTCCTG	24
4	*Casp1*	GTCTTGGAGACATCCTGTCAGG	GCATCTGTAGCCTAAATTCTGG	32
5	*Ccnf*	AGCACAAAGCCTTGCCACCATC	AAGCCAGGTGCGTGTCCTTGTC	25
6	*Ccng1*	TGGCCGAGATTTGACCTTCTGG	GTGCTTCAGTTGCCGTGCAGTG	22
7	*Ccng2*	GCCATCAAGCTAGGACTGTTAG	CACTTATCAACTCCATTCCCTG	26
8	*Cdkn1a (p21)*	TCCCGTGGACAGTGAGCAGTTG	CGTCTCCGTGACGAAGTCAAAG	22
9	*Cyp1a1*	TGGCCGATCGGAGGTCTTTC	AAGTGTTCACAGCGGGCGTG	29
10	*Cyp1a2*	GATGCTCTTCGGCTTGGGAAAG	CCATAGTTGGGTGTCAGGTCCAC	20
11	*Cyp4a10*	AGCCACAAGGGCAGTGTTCAGG	CCAAGCGGCCATTGGAAGAAAG	23
12	*Cyp21a1*	TGTGCTGCCCTTAAAGAAGAGTG	TTGAGCATCCCGTTCCCGTTTC	25
13	*Dpyd*	GTGCGGCTAAAGGCTGATGTGG	CCCATGGTTCACTGGTTTGCATG	24
14	*Egfr*	AGAACGCCTTCCACAGCCAC	ACTCTCGGAACTTTGGGCGG	22
15	*Ephx1*	CATTGTCTCCTCCCAGCGCTTC	GGGCATGCAGGATCTCAGAAGG	21
16	*Fabp5*	ACGGTCTGCACCTTCCAAGACG	ACCCGAGTGCAGGTGGCATTG	24
17	*Fos*	GTCGACCTAGGGAGGACCTTAC	CATCTCTGGAAGAGGTGAGGAC	31
18	*Gadd45b*	TGTACGAGGCGGCCAAACTG	TGTCGCAGCAGAACGACTGG	28
19	*Gadd45g*	GGAAAGCACAGCCAGGATGCAG	ATTCAGGACTTTGGCGGACTCG	26
20	*Gapdh*	GCTCTCAATGACAACTTTGTCAAG	CTTCCTTGGAGGCCATGTAGGC	22
21	*Gdf15*	AGCTGGAACTGCGCTTACGGG	CTCCAGCCCAAGTCTTCAAGAG	28
22	*Glul*	GGAATGGAGCAGGAATATACTC	ACCGCAGTAATACGGGCCTTG	22
23	*Gstk1*	CGTACTCCTGGCTGGGGCTTTG	CAGGTGGTTGGTTGCCGCTGTC	24
24	*Gyk*	GCCTGAAACAACTGCACTAGGC	CACAGCTTTCTTCCATGTGGAG	27
25	*Hist1h1c*	CGAGCTCATCACCAAGGCTGTG	CCCTTGCTCACCAGGCTCTTC	26
26	*Hspa1b (Hsp70)*	GACAAGTCGGAGAACGTGCAG	CGAGTAGGTGGTGAAGGTCTG	25
27	*Hspb1*	CGGTGCTTCACCCGGAAATAC	GCTGACTGCGTGACTGCTTTGG	25
28	*Hspb2 (Hsp27)*	CTCACAGTGAAGACCAAGGAAG	GGATAGGGAAGAGGACACTAGG	26
29	*Hmox1*	AAGACCGCCTTCCTGCTCAAC	CGAAGTGACGCCATCTGTGAGG	28
30	*Hprt1*	CTTGCTCGAGATGTCATGAAGGAG	TAATCCAGCAGGTCAGCAAAGAAC	26
31	*Igfbp1*	GATCAGCCCATCCTGTGGAACG	TTCTCGTTGGCAGGGCTCCTTC	24
32	*Isg20l1*	TTGAAGGGCAAGGTGGTGGTG	GAGCAGGTTTGGGACATAAGTG	24
33	*Jun*	GCCAAGAACTCGGACCTTCTC	AGTGGTGATGTGCCCATTGCTG	23
34	*Kras*	GGCAAGAGCGCCTTGACGATAC	TGGTCCCTCATTGCACTGTACTCC	28
35	*Lig3*	TGCGGCTCTACTTGCCACCTTC	CATGTGTGGCTGAGCCCATGTC	27
36	*Lrp1*	GGGCCATGAATGTGGAAATTGG	GTGGCATACACTGGGTTGGTG	22
37	*Mbd1*	GGATCCTGACACTCAAGAATGG	GTTTGGGCTAACACAGGAAGAG	23
38	*Mdm2*	TTGATCCGAGCCTGGGTCTGTG	AAGATCCTGATGCGAGGGCGTC	27
39	*Myc*	B5,GTCAGCAACAACCGCAAGTGCTC	AAAGCTGCGCTTCAGCTCGTTC	32
40	*Net1*	GACCTCCACGAAGAGTGTGAAG	CTGTACACTGGAGCCACAATCC	27
41	*Pdgfb*	AAGACGCGCACAGAGGTGTTCC	GGCATTGCACATTGCGGTTATTG	33
42	*Plk2*	CTGTTGAGAGCGTCTTCAGTTG	CCATAGTTCACAGTTAAGCAGC	28
43	*Pml*	GGCAAGAAGCGTCCTTACCTTC	GGACAGCAACAGCAGTTCAGTC	28
44	*Pmm1*	TGTCCCGAGGAGGCATGATAAG	CAAAGTCATTCCCGCCAGGAC	30
45	*Ppp1r3c*	TGGAAACCTGACGGAGTGCAG	GCAAGCCTTGGACTGCCAAAG	24
46	*Rad52*	TGACGCCACTCACCAGAGGAAG	GCTGGAAGTACCGCATGCTTGG	30
47	*Rcan1*	GGTCCACGTGTGTGAGAGTG	TGGATGGGTGTGTACTCCGG	24
48	*Trp53*	TTGGACCCTGGCACCTACAATG	GCAGACAGGCTTTGCAGAATGG	26
49	*Tubb2c*	TTGGCAACAGCACCGCTATTC	TCGGACACCAGGTCGTTCATG	23
50	*Ube2e1 (UbcM3)*	AACTGGAGCCCAGCCCTAACC	TGGCCATTCTGTCGTGTTCTGC	24
51	*Ung*	AACCTGAGTGGCCTCGTCTTCC	TCTGCATCCCAGGAACCCTCTG	29

Ct values are those of the highest group in the present experimental condition.

At 28 days, three DEN-28 d-Grp-1 genes showed a dose-dependent increase of more than four-fold. Seventeen DEN-28 d-Grp-2 genes were suggested to have a gradual dose-dependent increase, though less than that for the expression in DEN-28 d-Grp-1. Ungrouped *Igfbp1* showed a dose-dependent decrease of less than 0.3-fold.

Unsupervised *k*-means clustering results are shown in Fig. 3A. Genes were classified into four clusters based on the hierarchical clustering results. Gene expression was classified into four clusters (DEN-4 h-Cluster-1 to DEN-4 h-Cluster-4) 4 h after administration, and four clusters (DEN-28 d-Cluster-1 to DEN-28 d-Cluster-4) 28 days after administration. As unsupervised *k*-means clustering was performed for 4 h and 28-day data separately, cluster member genes were different for 4 h and 28 days.

At 4 h, all 12 DEN-4 h-Cluster-1 genes exhibited a dose-dependent increase of more than eight-fold. Fourteen DEN-4 h-Cluster-2 genes showed a gradual dose-dependent increase as compared to DEN-4 h-Cluster-1 genes. Although *Myc* and *Igfbp1* in DEN-4 h-Cluster-3 had some atypical dose–response, they showed an increase of up to or greater than two-fold, as a whole. Two genes in DEN-4 h-Cluster-4 exhibited a dose-dependent decrease of less than 0.3-fold [*Cyp1a2* and *Glul*]. For 28-day data, 4 DEN-28 d-Cluster-1 genes showed a dose-dependent increase of more than two-fold. *Igfbp1* in DEN-28 d-Cluster-3 showed a dose-dependent decrease of less than 0.3-fold.

Two types of clustering results for the DEN data are summarized as follows. A total of 28 genes showed a dose-dependent increase or decrease at 4 h or 28 days after administration. Twenty-six genes in DEN-4 h-Grp-1 or DEN-4 h-Grp-2 and DEN-4 h-Cluster-1, DEN-4 h-Cluster-2 or DEN-4 h-Cluster-3 showed a dose-dependent increase ranging from 2-fold to more than 64-fold [*Bax*, *Btg2*, *Ccng1*, *Ccng2*, *Cdkn1a*, *Cyp4a10*, *Cyp21a1*, *Fos*, *Gadd45b*, *Gdf15*, *Hspb1*, *Hmox1*, *Hsp27*, *Igfbp1*, *Isg20l1*, *Jun*, *Mbd1*, *Mdm2*, *Myc*, *Net1*, *Plk2*, *Pmm1*, *Ppp1r3c*, *Rad52*, *Rcan1* and *Tubb2c*]. Two genes in DEN-4 h-Grp-4

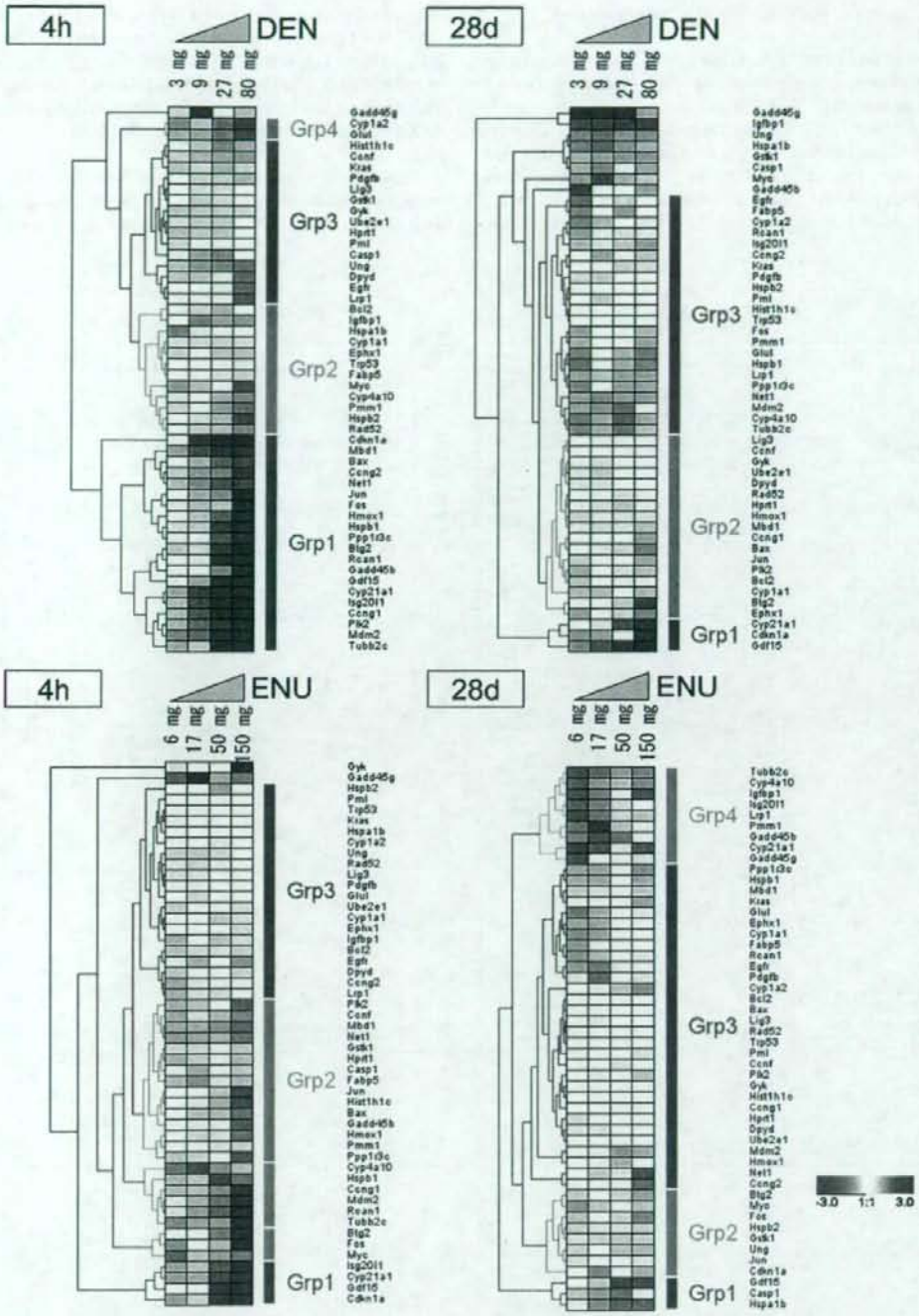

Fig. 2. Cluster analysis of gene expression after DEN and ENU treatment. The expression of 50 genes was clustered by hierarchical clustering after DEN or ENU treatment. Results of 4 h and 28 days were analyzed separately. The color displays show the $\log_2$ (expression ratio) as (1) red when the treatment sample is up-regulated relative to the control sample, (2) blue when the treatment sample is down-regulated relative to the control sample and (3) white when the $\log_2$ (expression ratio) is close to zero.

and DEN-4 h-Cluster-4 showed a dose-dependent decrease of less than 0.3-fold [*Cyp1a2* and *Glul*].

At 28 days, four genes in DEN-28 d-Grp-1 or DEN-28 d-Grp-2 and DEN-28 d-Cluster-1, which showed a dose-dependent increase at 4 h, also showed a dose-dependent increase by more than 2–4-fold [*Btg2*, *Cdkn1a*, *Cyp21a1* and *Gdf15*]. *Igfbp1* in the ungrouped group and DEN-28 d-Cluster-3 showed a dose-dependent decrease of less than 0.3-fold.

3.1.2. Identification of biologically relevant networks for DEN treatment

DEN numerical data of all 51 examined genes were analyzed by IPA, and 5 gene networks were extracted (Table 3). Five networks are also shown as bar graphs in Fig. 4.

For the 4 h time point, 35 genes were extracted in DEN-4 h-Network-1 (cancer, cell cycle and reproductive system disease); of these, 15 genes were examined in this study, and 11 of these genes showed a dose-dependent response [*Bax, Btg2, Ccng1, Cdkn1a, Gadd45b, Gdf15, Hspb1, Hspb2, Mdm2, Plk2* and *Pmm1*] (Fig. 4A, Network-1). Network-1 was a highly active network for DEN-4 h. *Trp53* and *Cdkn1a* appeared to be core genes in DEN-4 h-Network-1. *Trp53* has 15 associations [*Bax, Btg2, Casp1, Ccng1; Cdkn1a, Gadd45 complex, Gdf15, Hist1h1c, Hspb1, Mdm2, Plk2, Pml, Pmm1, Pdgf* complex and *Caspase* complex], and *Cdkn1a* has 9 associations [*Trp53, Plk2, Pdgf complex, Gdf15, Gadd45b, Gadd45g, Mdm2, Caspase* complex and *Pml*].

DEN-4 h-Network-2 (cell cycle, DNA replication, recombination, repair and cell death) consisted of 35 genes, 15 of which were examined in this study; 11 of these genes showed a dose-dependent

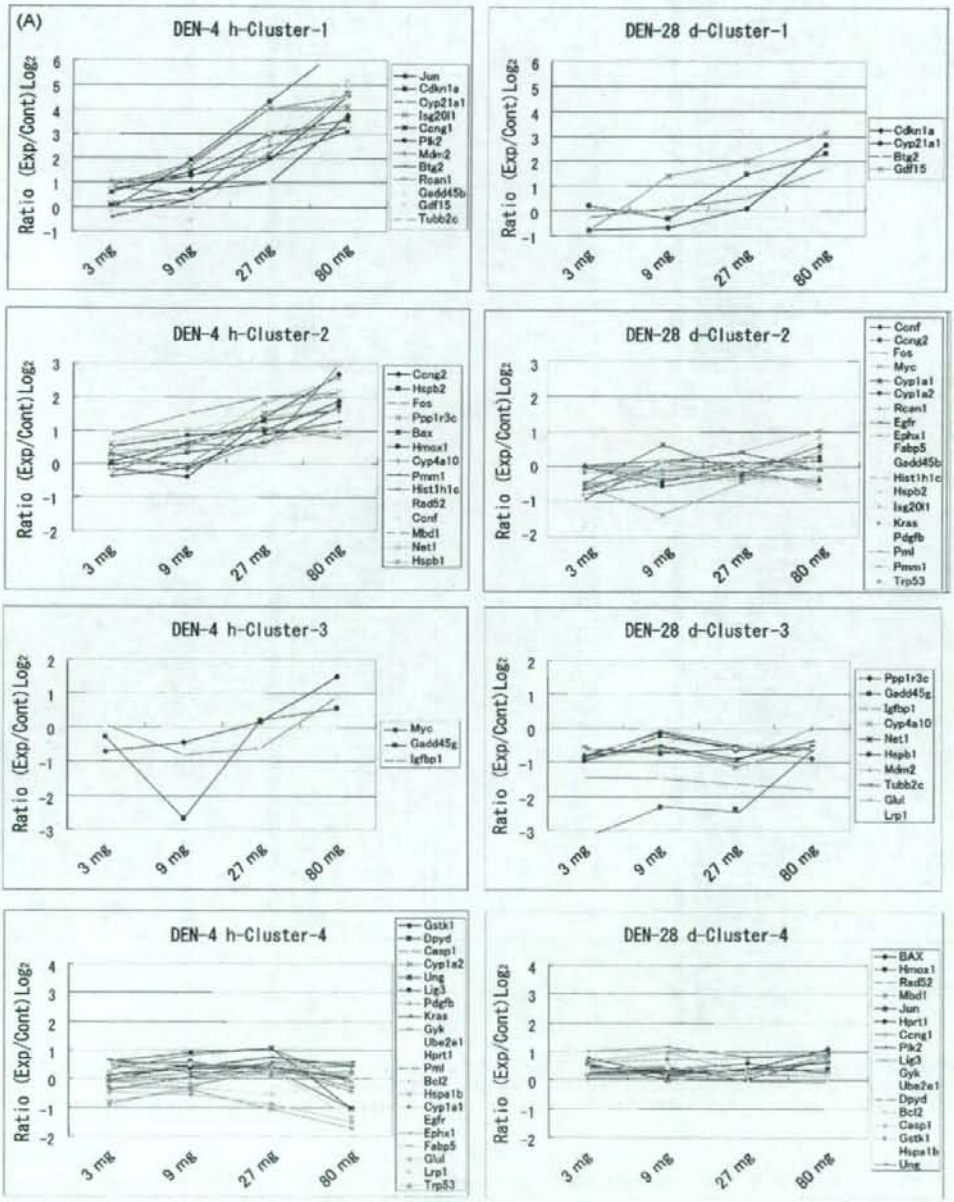

Fig. 3. Cluster analysis and dose-dependent expression pattern. The expression of 50 genes was clustered by *k*-means clustering after (A) DEN or (B) ENU treatment. Results of 4 h and 28 days were analyzed separately.

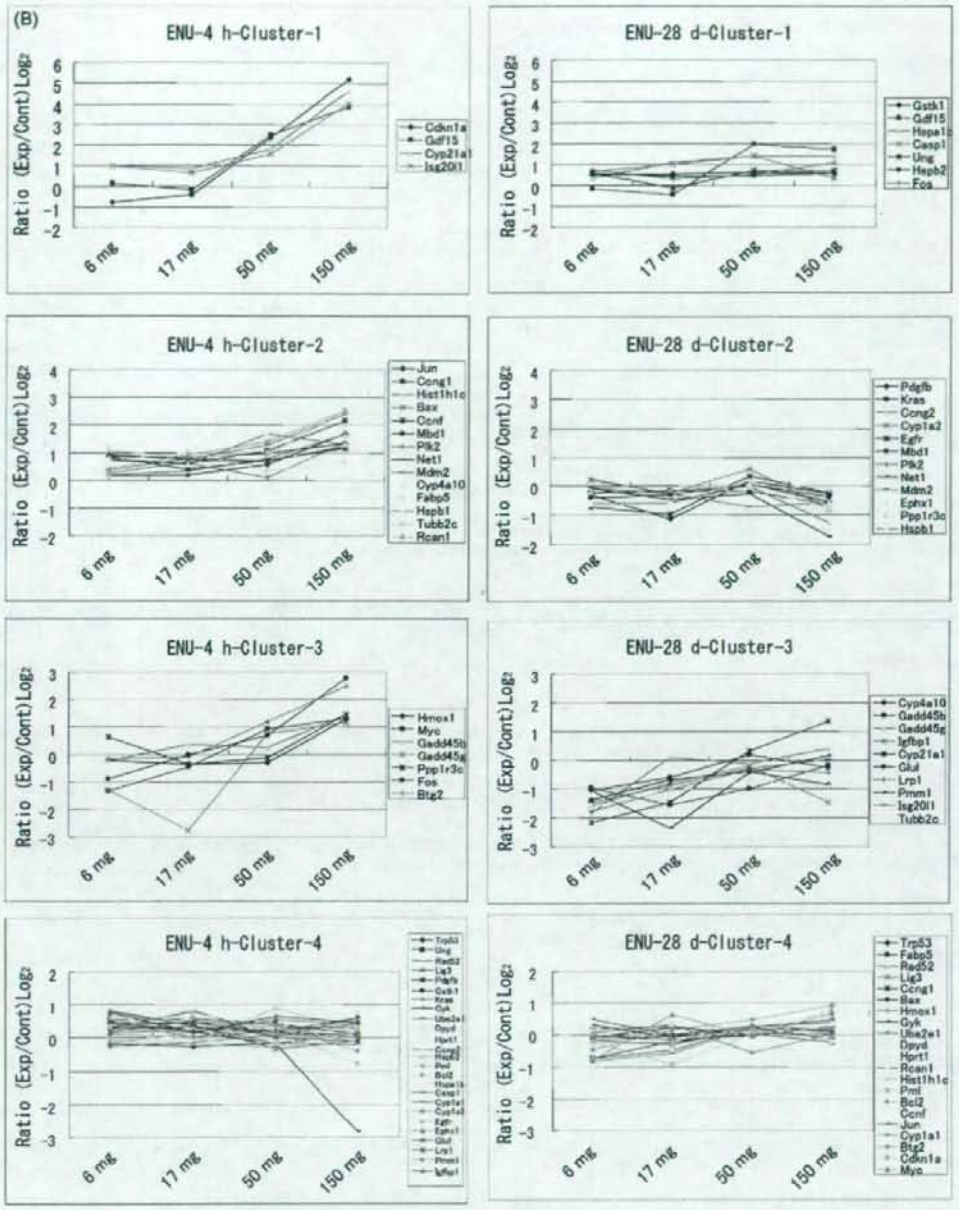

Fig. 3. (*Continued*).

response [*Ccng2*, *Cyp1a2*, *Cyp4a10*, *Cyp21a1*, *Gdf15*, *Glul*, *Igfbp1*, *Ppp1r3c Rad52*, *Rcan1* and *Tubb2c*] (Fig. 4A, Network-2). Network-2 was also a highly active network for DEN-4 h. *Il1b* and *Sp1* seemed to be core genes in DEN-4 h-Network-2. *Il1b* has five associations [*Gdf15*, *Fabp5*, *Rcan1*, *Igfbp1* and *Hprt1*], and *Sp1* has three associations [*Gdf15*, *Igfbp1* and *Cyp21a1*].

DEN-4 h-Network-3 (liver necrosis/cell death and hepatic system disease) consisted of 36 genes, 10 of which were examined in this study; 5 of these genes showed a dose-dependent response [*Fos*, *Hmox1*, *Jun*, *Myc* and *Net1*) (Fig. 4A, Network-3).

DEN-4 h-Network-4 (cell cycle, DNA replication, recombination, repair and cell death) consisted of 35 genes, 9 of which were examined in this study; 2 of these genes [*Isg20l1* and *Mbd1*] showed a dose-dependent response (Fig. 4A, Network-4).

DEN-4 h-Network-5 (cancer, drug metabolism and genetic disorder) consisted of two genes, neither of which showed a dose-dependent response in this study (Fig. 4A, Network-5).

For 28-day data, DEN-28 d-Network-1 consisted of the same genes and the same top functions as for DEN-4 h-Network-1 (Table 3(B)); however, a generally lower dose-dependent response

Table 3
Gene networks and their primary functions after DEN and ENU treatment.

Networks	Molecules in network	Top functions
(A) DEN 4 h		
1	Adaptor protein 2, Ahr-aryl hydrocarbon-*Arnt*, *Arf*, ***Bax***, ***Btg2***, *Casp1*, Caspase, *Cbp/p300*, ***Ccng1***, ***Cdkn1a***, *Creb*, Cyclin A, Cyclin E, *E2f*, *Erk1/2*, *Gadd45*, ***Gadd45b***, *Gadd45g*, ***Gdf15***, *Gsk3*, *Hist1h1c*, ***Hspb1***, ***Hspb2***, *Jun/Junb/Jund*, ***Mdm2***, *Mek1/2*, *Pak*, *Pdgf*, ***Plk2***, *Pml*, ***Pmm1***, *Pp2a*, *Rb*, *Stat*, *Trp53*	Cancer, Cell cycle, reproductive system disease
2	*Aatf*, *Aldh3a1*, *App*, beta-estradiol, *Ccne2*, ***Ccng2***, ***Cyp1a2***, ***Cpy21a1***, ***Cyp4a10***, *E2F1*, *Fabp5*, ***Gdf15***, *Gyk*, ***Glul***, *Hprt1*, *Hspa1b*, ***Igfbp1***, *Igfbp7*, *Il10*, *Il1b*, *Irf2*, *Klf10*, *MAZ*, *Meis1*, *Muc2*, ***Ppp1r3c***, ***Rad52***, ***Rcan1***, retinoic acid, *Scye1*, *Sp1*, *St8sia1*, *Tgm1*, *TopbpP1*, ***Tubb2c***	Cell cycle, DNA replication, recombination, and repair, cell death
3	*Akt*, *Ap1*, *Bcl2*, Calpain, *Egfr*, *Fgf*, ***Fos***, *Fos-Jun*, ***Hmox1***, *Ige*, *Il1*, *Jnk*, ***Jun***, *Kras*, *Lig3*, *Mapk*, *Mek*, *Mmp*, ***Myc***, ***Net1***, *P38*, *Mapk*, *Pdgf bb*, *Pdgfb*, *Pi3k*, *Pkc(s)*, *Pkg*, *Rar*, *Ras*, *Ras homolog*, *Rock*, *Rxr*, *Sos*, *Stat5a/b*, *Tgf beta*, *Vegf*	Cell death, hepatic system disease, liver necrosis/cell death
4	4-Phenylbutyric acid, *14-3-3*, Calmodulin, *Ccnf*, *Cdkn2a*, *Ck2*, *Cult1*, Cyclin D, *Cyp1a1*, *Ephx1*, *Hlra*, Histone h3, *Hnrpa2b1*, *Hsp70*, *Hsp90*, *Hspa1b*, hydrogen peroxide, *Ifng*, *Irf2*, ***Isg20l1***, lipoxin A4, *Lrp1*, ***Mbd1***, *Mcm2*, *Mcm3*, *Meis1*, *Pdk1*, *Pka*, RNA polymerase II, *Ssrp1*, *Supt16h*, *Tp53inp1*, *Ube2e1*, Ubiquitin, *Ung*	Cell cycle, DNA replication, recombination, and repair, cell death
5	*Cdh3*, D *Dpyd*	Cancer, drug metabolism, genetic disorder
(B) DEN 28 d		
1	Adaptor protein 2, Ahr-aryl hydrocarbon-*Arnt*, *Arf*, *Bax*, ***Btg2***, *Casp1*, Caspase, *Cbp/p300*, *Ccng1*, ***Cdkn1a***, *Creb*, Cyclin A, Cyclin E, *E2f*, *Erk1/2*, *Gadd45*, *Gadd45b*, *Gadd45g*, ***Gdf15***, *Gsk3*, *Hist1h1c*, *Hspb1*, *Hspb2*, *Jun/Junb/Jund*, *Mdm2*, *Mek1/2*, *Pak*, *Pdgf*, *Plk2*, *Pml*, *Pmm1*, *Pp2a*, *Rb*, *Stat*, *Trp53*	Cancer, cell cycle, reproductive system disease
2	*Aatf*, *Aldh3a1*, *App*, beta-estradiol, *Ccng2*, *Cyp1a2*, ***Cyp21a1***, *Cyp4a10* (includes EG:1579), *E2f1*, *Fabp5*, ***Gdf15***, *Gyk*, *Glul*, *Hrpt1*, *Hspa1b*, ***Igfbp1***, *Il10*, *Il1b*, *Klf10*, *Klk5*, *Maz*, *Meis1*, *Mt1e*, *Muc2*, *Nr4a3*, *Ppp1r3c*, *Rad52*, *Rcan1*, retinoic acid, *Scye1*, *Sp1*, *St8sia1*, *Tgm1*, *Topbp1*, *Tubb2c*	DNA replication, recombination, and repair, cell death, cell cycle
3	*Akt*, *Ap1*, *Bcl2*, Calpain, *Egfr*, *Fgf*, *Fos*, *Fos-Jun*, *Hmox1*, *Ige*, *Il1*, *Jnk*, *Jun*, *Kras*, *Lig3*, *Mapk*, *Mek*, *Mmp*, *Myc*, *Net1*, *P38 Mapk*, *Pdgf bb*, *Pdgfb*, *Pi3k*, *Pkc(s)*, *Pkg*, *Rar*, *Ras*, *Ras homolog*, *Rock*, *Rxr*, *Sos*, *Stat5a/b*, *Tgf beta*, *Vegf*	Cell death, hepatic system disease, liver necrosis/cell death
4	*14-3-3*, *Bag4*, Calmodulin, *Ccnf*, *Cdkn2a*, *Ck2*, *Cutl1*, *Cyp1a1*, *Dynlrb1*, *Ephx1*, *Hira*, Histone h3, *Hnrpa2b1*, *Hoxb9*, *Hsp70*, *Hsp90*, *Hspa1b*, hydrogen peroxide, *Ifng*, *Isg20l1*, *Lrp1*, *Mbd1*, *Meis1*, *Nol3*, *Pdk1*, *Pka*, *Ppfibp1*, RNA pol2-transcription factor, RNA polymerase II, *Smtn*, *Supt16h*, *Tp53inp1*, *Ube2e1*, Ubiquitin, *Ung*	Cellular development, cellular growth and proliferation, connective tissue development and function
5	*Cdh3*, *Dpyd*	Cancer, drug metabolism, genetic disorder
(C) ENU 4 h		
1	Adaptor protein 2, Ahr-aryl hydrocarbon-*Arnt*, *Arf*, ***Bax***, ***Btg2***, *Casp1*, Caspase, *Cbp/p300*, ***Ccng1***, ***Cdkn1a***, *Creb*, Cyclin A, Cyclin E, *E2f*, *Erk1/2*, *Gadd45*, ***Gadd45b***, *Gadd45g*, ***Gdf15***, *Gsk3*, ***Hist1h1c***, ***Hspb1***, *Hspb2*, *Jun/Junb/Jund*, ***Mdm2***, *Mek1/2*, *Pak*, *Pdgf*, ***Plk2***, *Pml*, *Pmm1*, *Pp2a*, *Rb*, *Stat*, *Trp53*	Cancer, cell cycle, reproductive system disease
2	*Aatf*, *Aldh3a1*, *App*, *Apphp1*, beta-estradiol, *Ccne2*, *Ccng2*, *Cyp1a2*, ***Cyp21a1***, ***Cyp4a10***, *E2f1*, ***Fabp5***, ***Gdf15***, *Gyk*, *Glul*, *Hprt1*, *Hdps1b*, *Igfbp1*, *Il10*, *Il1b*, *Klf10*, *Maz*, *Mis1*, *Muc2*, *Nr4a3*, ***Ppp1r3c***, *Rad52*, ***Rcan1***, retinoic acid, *Scye1*, *Sp1*, *St8sia1*, *Tgm1*, *Topbp1*, ***Tubb2c***	DNA replication, recombination, and repair, cell cycle, cell signaling
3	*Akt*, *Ap1*, *Bcl2*, Calpain, *Egfr*, *Fgf*, ***Fos***, *Fos-Jun*, ***Hmox1***, *Ige*, *IL1*, *Jnk*, ***Jun***, *Kras*, *Lig3*, *Mapk*, *Mek*, *Mmp*, ***Myc***, ***Net1***, *P38*, *Mapk*, *Pdgf bb*, *Pdgfb*, *Pi3k*, *Pkc(s)*, *Pkg*, *Rar*, *Ras*, *Ras homolog*, *Rock*, *Rxr*, *Sos*, *Stat5a/b*, *Tgf beta*, *Vegf*	Cell death, hepatic system disease, liver necrosis/cell death
4	4-phenylbutyric acid, *14-3-3*, Calmodulin, ***Ccnf***, *Cdkn2a*, *Ck2*, *Cult1*, Cyclin D, *Cyp1a1*, *Ephx1*, *Hlra*, Histone h3, *Hnrpa2b1*, *Hsp70*, *Hsp90*, *Hspa1b*, hydrogen peroxide, *Ifng*, *Irf2*, ***Isg20l1***, lipoxin A4, *Lrp1*, ***Mbd1***, *Mcm2*, *Mcm3*, *Meis1*, *Pdk1*, *Pka*, RNA polymerase II, *Ssrp1*, *Supt16h*, *Tp53inp1*, *Ube2e1*, Ubiquitin, *Ung*	Cell cycle, DNA replication, recombination, and repair, cell death
5	*Cdh3*, *Dpyd*	Cancer, drug metabolism, genetic disorder
(D) ENU 28 d		
1	Adaptor protein 2, Ahr-aryl hydrocarbon-*Arnt*, *Arf*, *Bax*, *Btg2*, ***Casp1***, Caspase, *Cbp/p300*, *Ccng1*, *Cdkn1a*, *Creb*, Cyclin A, Cyclin E, *E2f*, *Erk1/2*, *Gadd45*, *Gadd45b*, *Gadd45g*, ***Gdf15***, *Gsk3*, *Hist1h1c*, *Hspb1*, ***Hspb2***, *Jun/Junb/Jund*, *Mdm2*, *Mek1/2*, *Pak*, *Pdgf*, *Plk2*, *Pml*, *Pmm1*, *Pp2a*, *Rb*, *Stat*, *Trp53*	Cancer, cell cycle, reproductive system disease
2	*Aatf*, Ahr-aryl hydrocarbon, *App*, *Apphp1*, beta-estradiol, *Ccng2*, *Cd68*, *Cdc45l*, *Cyp1a2*, *Cyp21a1*, *Cyp4a10*, *E2f1*, *Fabp5*, *Folr2*, ***Gdf15***, *Gyk*, *Glul*, *Hprt1*, ***Hspa1b***, *Igfbp1*, *Il10*, *Il1b*, *Klk5*, *Krt16*, *Nr4a3*, *Ppp1r3c*, *Rad52*, *Rcan1*, retinoic acid, *Rrs4x*, *Serpinb9*, *Sp1*, *TacstdA1*, *Tspo*, *Tubb2c*	Cell signaling, molecular transport, small molecule biochemistry
3	*Akt*, *Ap1*, *Bcl2*, Calpain, *Egfr*, *Fgf*, ***Fos***, *Fos-Jun*, *Hmox1*, *Ige*, *IL1*, *Jnk*, *Jun*, *Kras*, *Lig3*, *Mapk*, *Mek*, *Mmp*, *Myc*, ***Net1***, *P38*, *Mapk*, *Pdgf bb*, *Pdgfb*, *Pi3k*, *Pkc(s)*, *Pkg*, *Rar*, *Ras*, *Ras homolog*, *Rock*, *Rxr*, *Sos*, *Stat5a/b*, *Tgf beta*, *Vegf*	Cell death, hepatic system disease, liver necrosis/cell death
4	*14-3-3*, *Aco1*, *Asf1b*, *Bag4*, Calmodulin, *Ccnf*, *Cdkn2a*, *Ck2*, *Cyp1a1*, *Dynlrb1*, *Ephx1*, *Hira*, Histone h3, *Hoxb9*, *Hsp70*, *Hsp90*, ***Hspa1b***, hydrogen peroxide, *Ifng*, *Isg20l1*, *Lamp1*, *Lrp1*, *Mbd1*, *Nol3*, *Pka*, *Ppfibp1*, RNA pol2-transcription factor, RNA polymerase II, *Rpl21*, *Smtn*, *Sncg*, *Supt16h*, *Ube2e1*, Ubiquitin, ***Ung***	Cellular development, cellular growth and proliferation, connective tissue development and function
5	*Cdh3*, *Dpyd*	Cancer, drug metabolism, genetic disorder

Biologically relevant networks extracted by IPA are shown for gene expression data after (A) DEN-4 h, (B) DEN-28 d, (C) ENU-4 h or (D) ENU-28 d treatment. Bold underlined genes show dose-dependent expression. Thin underlined genes are genes examined in the present study. *Pdgf bb* in Network-3 means *Pdgf* groups of *Pdgfa*, *Pdgfb*, *Pdgfc* and *Pdgfd*. *Hsp70* in Network-4 means *Hsp* groups of *Hspa14 hspa1a*, *Hspa1b*, *Hspa1l*, *Hspa2*, *Hspa4 hspa5*, *Hspa6*, *Hspa7*, *Hspa8*, and *Hspa9*.

was observed, and only *Btg2*, *Cdkn1a* and *Gdf15* showed a dose-dependent increase (Fig. 4A, Network-1). DEN-28 d-Network-2 included several different genes from those in DEN-4 h-Network-2 but had the same primary functions as for DEN-4 h-Network-2, and *Cyp21a1*, *Gdf15* and *Igfbp1* exhibited dose-dependency (Fig. 4A, Network-2). DEN-28 d-Network-3 consisted of the same genes and the same primary functions as for DEN-4 h-Network-3; however, no genes showed dose-dependency (Fig. 4A, Network-3). DEN-28 d-Network-4 contained a few different genes and primary functions from those of DEN-4 h-Network-4, but no genes showed a dose

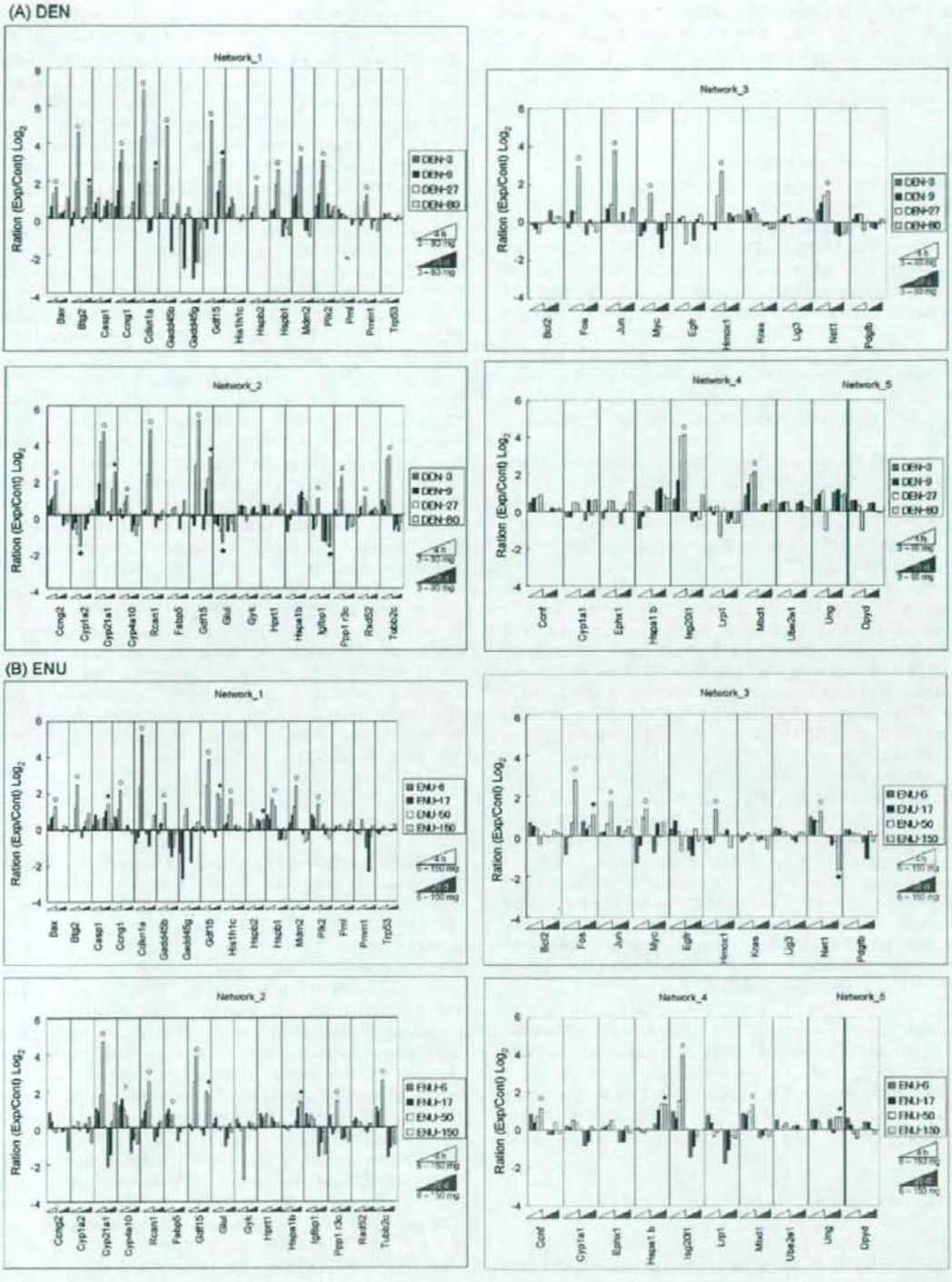

Fig. 4. Dose-dependent gene expression in each network based on different time points. The ratio values (log_2) of genes in each network are shown as bar graphs for DEN treatment (A) or ENU treatment (B). ○ shows a dose-dependent increase at 4 h, ♦ shows a dose-dependent increase at 28 days and ● shows a dose-dependent decrease.

response. DEN-28 d-Network-5 consisted of the same genes and the same top functions as those of DEN-4 h-Network-5, with no genes showing dose-dependency in this study (Fig. 4A, Network-5).

3.2. Dose-dependent alteration of gene expression induced with ENU

3.2.1. Clustering analysis for gene expression

Unsupervised hierarchical clustering results are shown in Fig. 2. The clustering presented three groups (ENU-4 h-Grp-1 to ENU-4 h-Grp-3) and two ungrouped genes for the 4 h time point after administration and four groups (ENU-28 d-Grp-1 to ENU-28 d-Grp-4) for the 28-day time point after administration. As unsupervised hierarchical clustering was performed on 4 h and 28-day data separately, group member genes were different between these two groups.

All four ENU-4 h-Grp-1 genes showed a dose-dependent increase by more than 16–32-fold 4 h after administration. Twenty-four ENU-4 h-Grp-2 genes were suggested to have a gradual dose-dependent increase of less than that of the expression in ENU-4 h-Grp-1.

All three ENU-28 d-Grp-1 genes showed a dose-dependent increase by more than two-fold 28 days after administration. Eight ENU-28 d-Grp-2 genes were suggested to have a gradual dose-dependent increase of less than that of the expression in ENU-28 d-Grp-1. *Net1* in ENU-28 d-Grp-3 showed a dose-dependent decrease of less than 0.3-fold.

Unsupervised *k*-means clustering results are shown in Fig. 3B. In the same way as for DEN, we classified these genes into four clusters based on hierarchical clustering results. For 4 h, four ENU-4 h-Cluster-1 genes exhibited a dose-dependent increase by more than 16-fold. Fourteen ENU-4 h-Cluster-2 genes exhibited a gradual dose-dependent increase as compared to genes in ENU-4 h-Cluster-1. Seven ENU-4 h-Cluster-3 genes showed an increase as a whole, with some atypical features. For 28-day data, seven ENU-28 d-Cluster-1 genes were suggested to have a tendency for a dose-dependent increase. *Net1* in ENU-28 d-Cluster-2 showed a dose-dependent decrease of less than 0.3-fold.

Two kinds of clustering results of ENU treatment are summarized as follows. A total of 29 genes showed a dose-dependent increase or decrease at 4 h or 28 days after administration. For 4 h, a total of 24 genes in ENU-4 h-Grp-1 or ENU-4 h-Grp-2 and ENU-4 h-Cluster-1, ENU-4 h-Cluster-2 or ENU-4 h-Cluster-3 showed a dose-dependent increase ranging from 2-fold to more than 32-fold [*Bax, Btg2, Ccng1, Ccnf, Cdkn1a, Cyp4a10, Cyp21a1, Fabp5, Fos, Gadd45b, Gdf15, Hist1h1c, Hmox1, Hspb1, Isg20l1, Jun, Mbd1, Mdm2, Myc, Net1, Plk2, Ppp1r3c, Rcan1* and *Tubb2c*].

For 28 days, a total of eight genes were classified as dose–response genes. Four genes in ENU-28 d-Grp-1, ENU-28 d-Grp-2, and ENU-28 d-Cluster-1 showed a dose-dependent increase of more than 2-fold [*Casp1, Fos, Gdf15* and *Hspa1b*]. Another three genes in ENU-28 d-Grp2 and ENU-28 d-Cluster-1 showed less than a two-fold increase [*Gstk1, Hspb2* and *Ung*]. *Net1* in ENU-28 d-Grp-3 and ENU-28 d-Cluster-2 showed a dose-dependent decrease of less than 0.3-fold.

3.2.2. Identification of biologically relevant networks for ENU treatment

ENU numerical data for all 51 examined genes were also analyzed by IPA for 4 h and 28-day data, and five gene networks were extracted (3). In total, the gene expression pattern for ENU was similar to the pattern for DEN; however, some differences were observed.

For 4 h, ENU-4 h-Network-1 consisted of the same genes and the same top functions as for DEN-4 h-Network-1, and 10 of these genes showed a dose-dependent increase [*Bax, Btg2, Ccng1, Cdkn1a, Gadd45b, Gdf15, Hist1h1c, Hspb1, Mdm2* and *Plk2*] (Fig. 4B, Network-1). Network-1 was the most active network for ENU-4 h. ENU-4 h-Network-2 (DNA replication, recombination, repair, cell cycle and cell signaling) included a different primary function from that of DEN-4 h-Network-2 and a few different genes from those for DEN, and seven genes showed a dose-dependent increase [*Cyp21a1, Cyp4a10, Fabp5, Gdf15, Ppp1r3c, Rcan1* and *Tubb2c*] (Fig. 4B, Network-2). ENU-4 h-Network-3 consisted of the same genes and the same top functions as those for DEN-4 h-Network-3, and five genes showed a dose-dependent increase [*Fos, Hmox1, Jun, Myc* and *Net1*] (Fig. 4B, Network-3). ENU-4 h-Network-4 also consisted of the same genes and the same top functions as those for DEN, and three genes showed a dose-dependent increase [*Ccnf, Isg20l1* and *Mbd1*] (Fig. 4B, Network-4). ENU-4 h-Network-5 consisted of the same genes and the same top functions as those for DEN-4 h-Network-5, but no genes showed a dose–response in this study (Fig. 4B, Network-5).

Network-1, Network-3 and Network-5 consisted of common genes and common top functions for both 4 h and 28 days and for both DEN and ENU. For 28 days, three genes in ENU-28 d-Network-1 showed a dose-dependent increase [*Casp1, Gdf15* and *Hspb2*] (Fig. 4B, Network-1). ENU-28 d-Network-2 included 10 different genes from those for ENU-4 h-Network-2 and had different top functions (cell signaling, molecular transport and small molecule biochemistry) from those of DEN-4 h-Network-2, DEN-28 d-Network-2 and ENU-4 h-Network-2, and 2 genes showed a dose-dependent increase [*Gdf15 and Hspa1b*] (Fig. 4B, Network-2). *Fos* and *Net1* in ENU-28 d-Network-3 showed a dose–response (Fig. 4B, Network-3). ENU-28 d-Network-4 (Table 2D) included different primary functions (cellular development, cellular growth, proliferation and connective tissue development and function) and 10 different genes from ENU-4 h-Network-4; two genes showed a dose–response [*Hspab1* and *Ung*]. ENU-28 d-Network-5 consisted of the same genes and the same top functions as those of DEN-4 h-Network-5, while no genes showed a dose–response in this study (Fig. 4A, Network-5).

4. Discussion

We examined the dose-dependency of gene expression changes for 51 genes in mouse liver treated with two *N*-nitroso genotoxic hepatocarcinogens, DEN and ENU, by qPCR at early times after administration. We selected 51 candidate genes based on our previous results of Affymetrix GeneChip Mu74AV2 and original DNA microarray of samples after treatment with DEN, dimethylnitrosamine, dipropylnitrosamine, ENU, *o*-aminoazotoluene, 7,12-dimethylbenz[*a*]anthracene, dibenzo[*a,l*]pyrene, phenobarbital and ethanol in our JEMS/MMS/Toxicogenomics group collaborative study. Because only a single dose was used for each chemical in the previous study, we examined dose-dependency in gene expression changes in this study using two representative chemicals. We showed distinct dose-dependency of gene expression changes induced by DEN and ENU; these changes associated with cancer, cell cycle arrest, DNA replication, recombination, repair and cell death not only at 4 h, but also, for some, at 28 days after administration. Similar gene expression changes between DEN and ENU were characteristic. Twenty-one genes exhibited a distinct dose-dependent increase at 4 h for both carcinogens [*Bax, Btg2, Ccng1, Cdkn1a, Cyp4a10, Cyp21a1, Fos, Gadd45b, Gdf15, Hmox1, Hspb1, Isg20l1, Jun, Mbd1, Mdm2, Myc, Net1, Plk2, Ppp1r3c, Rcan1* and *Tubb2c*], although the gene expression changed after ENU was generally weaker relative to that after DEN. The results were consistent with a previous report that showed more DNA lesions with DEN than with ENU a few hours after administration [6]. Only *Gdf15* showed a dose-dependent increase at 28 days for

both carcinogens. An additional seven different genes for DEN and eight genes for ENU also showed dose-dependency. *Ccng2*, *Hspb2*, *Igfbp1*, *Pmm1* and *Rad52* showed a dose-dependent increase and *Cyp1a2* and *Glul* showed a dose-dependent decrease 4 h after administration only with DEN. *Btg2*, *Cdkn1a* and *Cyp21a1* showed a dose-dependent increase 28 days after administration only with DEN and these genes also showed a dose–response at 4 h. *Ccnf*, *Fabp5* and *Hist1h1c* showed a dose-dependent increase 4 h after administration only with ENU. *Casp1*, *Fos*, *Gstk1*, *Hspa1b*, *Hspb2* and *Ung* showed a dose-dependent increase 28 days after administration only with ENU. *Ccnf* in DEN-4 h and *Bax* and *Ephx1* in DEN-28 d showed equivocal changes. We only observed several dose-dependent decreases in expression of genes [*Cyp1a2*, *Glul*, *Igfbp1* and *Net1*] after DEN and ENU in the present experimental conditions.

In the previous study [10], gene expression changes in number and degree were observed to peak at 4 h after administration and were lower at 20 h, 14 and 28 days. In the present study, we investigated the gene expression pattern at two different time points: 4 h, during production of many DNA lesions, and 28 days, during fixing of mutations [6]. We expected to observe the earliest and most varied effects in many cells in the liver, including DNA lesions, 4 h after administration. It was presumed that most of the DNA-damaged cells would be repaired, that some of the damaged cells would die and that only a few cells would progress to carcinogenesis. We reasoned that it would be useful to examine the earliest various effects to understand the potential gene-altering ability of carcinogens. The second time point, 28 days, is the time by which most mutations are fixed, the remainder of which would be related to carcinogenesis. We expected to observe gene expression changes which would reflect the effects of mutation at 28 days. The role of genes with altered expression might be different even if expression of the same gene was changed at 4 h and 28 days.

In addition, we examined gene networks using IPA to clarify interactions between genes with altered expression. IPA identified five networks of genes regulated at 4 h after DEN and ENU treatment (Table 3 and Fig. 4). As for DEN, 11 dose-dependent genes [*Bax*, *Btg2*, *Ccng1*, *Cdkn1a*, *Gadd45b*, *Gdf15*, *Hspb1*, *Hspb2*, *Mdm2*, *Plk2* and *Pmm1*] belonged to Network-1 (cancer and cell cycle) and the other 11 dose-dependent genes [*Ccng2*, *Cyp1a2*, *Cyp4a10*, *Cyp21a1*, *Gdf15*, *Glul*, *Igfbp1*, *Ppp1r3c Rad52*, *Rcan1* and *Tubb2c*] belonged to Network-2 (cell cycle, cell death, DNA replication, recombination and repair). In detail, *Gdf15* was extracted in both Network-1 and Network-2. As for ENU, 10 dose-dependent genes [*Bax*, *Btg2*, *Ccng1*, *Cdkn1a*, *Gadd45b*, *Gdf15*, *Hist1h1c*, *Hspb1*, *Mdm2* and *Plk2*] belonged to the same Network-1 and 7 dose-dependent genes [*Cyp21a1*, *Cyp4a10*, *Fabp5*, *Gdf15*, *Ppp1r3c*, *Rcan1* and *Tubb2c*] belonged to a different Network-2 (DNA replication, recombination and repair, and cell cycle and cell signaling). *Hspb2* and *Pmm1* showed dose–responses only in DEN-4 h-Network-1 and *Hist1h1c* showed a dose–response only in ENU-4 h-Network-1. [Cell death] in DEN-4 h-Network-2 was replaced with [Cell signaling] in ENU-4 h-Network-2. *Ccng2*, *Cyp1a2*, *Glul*, *Igfbp1* and *Rad52* showed dose–responses only in DEN-4 h-Network-2 and *Fabp5* showed a dose–response only in ENU-4 h-Network-2. This difference in Network-2 was the most remarkable difference between the effects of DEN and ENU in the present study. The top functions of Network-1 and Network-2 were characteristic networks for DEN-4 h and ENU-4 h, being typical of carcinogenic compounds. As for 28 days, IPA also identified five networks of genes, however, only a few genes showed a dose–response with DEN and ENU. As for DEN, three dose-dependent genes [*Btg2*, *Cdkn1a* and *Gdf15*] belonged to Network-1 and two genes [*Cyp21a1* and *Gdf15*] belonged to Network-2. As for ENU, three dose-dependent genes [*Casp1*, *Gdf15* and *Hspb2*] belonged to Network-1, [*Gdf15* and *Hspa1b*] belonged to Network-2, [*Fos* and *Net1*] belonged to Network-3 and [*Hspa1b* and *Ung*] belonged to Network-4. The present results suggested similar functions for *N*-nitroso carcinogens DEN and ENU, with several differences. We have examined effects of other genotoxic and non-genotoxic carcinogens in mouse liver at 4 h and have generated various networks for various carcinogens (unpublished).

We showed that Network-1 was associated with cancer and the cell cycle. To understand more detailed functions, we examined a major canonical pathway for each network. A major canonical pathway in Network-1 was *p53* signaling. The increase of *Cdkn1a*, *Ccng1* and *Gadd45* demonstrated cell cycle arrest. The expression pattern (Fig. 4) at 4 h showed that cell cycle arrest would proceed, to then be released by day 28. Both *p53* and *Bax* were associated with initiation of apoptosis.

In the same way, a major canonical pathway in Network-2 was aryl hydrocarbon receptor signaling [14]. Furthermore, aryl hydrocarbon receptor signaling as an adaptive response was manifested as the induction of xenobiotic metabolizing enzymes; *Cyp1a2*, *Cyp21a1* and *Cyp4a10* take part in this pathway. *Cyp21a1* also takes part in biosyntheses of steroid hormones [15]. Inflammation of the liver is controlled at 28 days after administration because steroid hormones function to suppress inflammation.

Growth/differentiation factor-15 (*Gdf15*) was the only gene whose expression increased at 4 h and 28 days of both DEN and ENU and belonged to Network-1 and Network-2 at 4 h and 28 days of DEN and ENU. *Gdf15* is a divergent Tgf-beta family member that is expressed following liver injury and carcinogen exposure [16]. *Gdf15* in liver is rapidly and dramatically up-regulated following various surgical and chemical treatments that cause acute liver injury and regeneration [17].

A major canonical pathway in Network-3 was platelet-derived growth factor (*Pdgf*) signaling. *Pdgfb*, *Kras*, *Jun*, *Fos* and *Myc* may be associated with *Pdgf* signaling. In this canonical pathway, *Pdgfb* phosphorylates other proteins and activates the downstream genes *Kras*, *Jun*, *Fos* and *Myc* [18–21], one reason why *Pdgfb* expression did not change significantly (Fig. 3A, Cluster-4).

Our results show that most differentially expressed genes at 4 h and 28 days exhibited a dose–response. Only a few genes, *Dpyd*, *Egfr*, *Lrp1* and *Ung* for DEN at 4 h; *Gyk* for ENU at 4 h; and *Ccng2* for ENU at 28 days showed atypical gene expression changes at the highest dose. These changes may be toxicity-related. *Dpyd* is associated with pyrimidine metabolism. *Egfr* is associated with cell proliferation. *Lrp* plays a clear protective role in atherogenesis. *Ung* is associated with DNA repair. Their decrease may show the loss of cell maintenance because hepatocytes will have received much lethal damage at the highest dose. *Gyk* is associated with xenobiotic metabolism signaling. It has been reported that glycerol kinase deficiency is involved in lipid metabolism, carbohydrate metabolism, and insulin signaling [22]. Indeed, it has been reported that type 2 diabetes is caused by ENU but not by DEN [23]. Unlike classical cyclins that promote cell cycle progression, cyclin G2 blocks cell cycle entry. The decrease of *Ccng2* mRNA may promote cell cycle progression.

Previously, we reported differential gene expression induced by two *N*-nitroso genotoxic hepatocarcinogens, DEN and dipropylnitrosamine (DPN) as compared to phenobarbital and ethanol in mouse liver examined with an original oligonucleotide microarray and qPCR [10]. We observed 11 differentially expressed genes 4 h after administration, including 7 tumor suppressor *Trp53* target genes, *Bax*, *Ccng1*, *Cdkn1a*, *Hspb2*/*Hsp27*, *Jun*, *Mdm2*, and *Plk2*/*Snk*; the other genes were *Ccnf*, *Hmox1*, *Mbd1*, and *Rad52*. Furthermore, some degree of differential gene expression of *Ccng1*, *Cdkn1a* and *Plk2*/*Snk* was observed 28 days after administration. In the present study, we selected 51 candidate genes (Table 1) based on our original DNA microarray and Affymetrix GeneChip Mu74AV2 data (not published) on seven genotoxic carcinogens, phenobarbital and ethanol. The present results show that 28 genes for

DEN and 29 genes for ENU exhibited dose-dependent differential expression. Differential gene expression was observed commonly at least for *Bax*, *Ccng1*, *Cdkn1a*, *Hmox1*, *Jun*, *Mbd1*, *Mdm2* and *Plk2* with these three *N*-nitroso carcinogens (DEN, DPN and ENU). As we expanded qPCR analysis from 14 genes in the previous study [10] to 51 genes in the present study, we could show complex gene networks by IPA. Twenty genes, *Btg2*, *Casp1*, *Ccng2*, *Cyp4a10*, *Cyp21a1*, *Ephx1*, *Gadd45b*, *Gdf15*, *Glul*, *Gstk1*, *Hspa1b*, *Hspb1*, *Igfbp1*, *Isg20l1*, *Net1*, *Pmm1*, *Ppp1r3c*, *Rcan1*, *Tubb2c* and *Ung*, which showed dose–responses in the present study, were newly examined.

We examined only pooled materials from five mice in the present study. However, we already reported that at least five genes (*Gapdh*, *Jun*, *Ccng1*, *Hspb2*/*Hsp27* and *Rad52*) exhibited only small inter-individual mouse gene expression variation [10] with DEN treatment after 4 h and 28 days. Additional study showed that *Bax*, *Hmox1*, *Mbd1*, *Mdm2* and *Plk2* also exhibited only small inter-individual gene expression variation with DEN treatment at 4 h and 28 days (unpublished data).

We will continue further studies on other types of chemicals for characterizing mutagenic and carcinogenic compounds; these data will be useful for chemical risk assessment and for furthering our understanding of the underlying biological processes.

Conflict of interest

We have not any conflicting interest include employment, consultancies, stock ownership, honoraria, paid expert testimony, patent applications/registrations, and grants or other funding.

Acknowledgements

This work was partly supported by KAKENHI (18310047) (C. Furihata, T. Watanabe and T. Suzuki), The Ministry of Education, Culture, Sports, Science and Technology, Japan and a High-Tech Research Center project for private universities with a matching fund subsidy from The Ministry of Education, Culture, Sports, Science and Technology, Japan (C. Furihata).

References

[1] B.A. Diwan, H. Meier, Carcinogenic effects of a single dose of diethylnitrosamine in three unrelated strains of mice: genetic dependence of the induced tumor types and incidence, Cancer Lett. 1 (1976) 249–253.
[2] A.P. Kyriazis, S.D. Vesselinovitch, Transplantability and biological behavior of mouse liver tumors induced by ethylnitrosourea, Cancer Res. 33 (1973) 332–338.
[3] J.A. Swenberg, M.C. Dyroff, M.A. Bedell, J.A. Popp, N. Huh, U. Kirstein, M.F. Rajewsky, O4-ethyldeoxythymidine, but not O6-ethyldeoxyguanosine, accumulates in hepatocyte DNA of rats exposed continuously to diethylnitrosamine, Proc. Natl. Acad. Sci. U.S.A. 81 (1984) 1692–1695.
[4] J.L. Yang, P.C. Lee, S.R. Lin, J.G. Lin, Comparison of mutation spectra induced by N-ethyl-N-nitrosourea in the hprt gene of Mer+ and Mer− diploid human fibroblasts, Carcinogenesis 15 (1994) 939–945.
[5] T. Suzuki, M. Hayashi, T. Sofuni, Initial experiences and future directions for transgenic mouse mutation assays, Mutat. Res. 307 (1994) 489–494.
[6] E.J. Mientjes, A. Luiten-Schuite, E. van der Wolf, Y. Borsboom, A. Bergmans, F. Berends, P.H. Lohman, R.A. Baan, J.H. van Delft, DNA adducts, mutant frequencies, and mutation spectra in various organs of lambda lacZ mice exposed to ethylating agents, Environ. Mol. Mutagen. 31 (1998) 18–31.
[7] J.F. Waring, R.A. Jolly, R. Ciurlionis, P.Y. Lum, J.T. Praestgaard, D.C. Morfitt, B. Buratto, C. Roberts, E. Schadt, R.G. Ulrich, Clustering of hepatotoxins based on mechanism of toxicity using gene expression profiles, Toxicol. Appl. Pharmacol. 175 (2001) 28–42.
[8] M.J. Bartosiewicz, D. Jenkins, S. Penn, J. Emery, A. Buckpitt, Unique gene expression patterns in liver and kidney associated with exposure to chemical toxicants, J. Pharmacol. Exp. Ther. 297 (2001) 895–905.
[9] M. Provenzano, S. Mocellin, Complementary techniques: validation of gene expression data by quantitative real time PCR, Adv. Exp. Med. Biol. 593 (2007) 66–73.
[10] T. Watanabe, K. Tobe, Y. Nakachi, Y. Kondoh, M. Nakajima, S. Hamada, C. Namiki, T. Suzuki, S. Maeda, A. Tadakuma, M. Sakurai, Y. Arai, A. Hyogo, M. Hoshino, T. Tashiro, H. Ito, H. Inazumi, Y. Sakaki, H. Tashiro, C. Furihata, Differential gene expression induced by two genotoxic *N*-nitroso carcinogens, phenobarbital and ethanol in mouse liver examined with oligonucleotide microarray and quantitative real-time PCR, Gene Environ. 29 (2007) 115–127.
[11] K. Sekihashi, A. Yamamoto, Y. Matsumura, S. Ueno, M. Watanabe-Akanuma, F. Kassie, S. Knasmüller, S. Tsuda, Y.F. Sasaki, Comparative investigation of multiple organs of mice and rats in the comet assay, Mutat. Res. 517 (2002) 53–75.
[12] S. Madle, S.W. Dean, U. Andrae, G. Brambilla, B. Burlinson, D.J. Doolittle, C. Furihata, T. Hertner, C.A. McQueen, H. Mori, Recommendations for the performance of UDS tests in vitro and in vivo, Mutat. Res. 312 (1994) 263–285.
[13] A. Sturn, J. Quackenbush, Z. Trajanoski, Genesis: Cluster analysis of microarray data, Bioinformatics 18 (2002) 207–208.
[14] D.W. Kim, L. Gazourian, S.A. Quadri, R. Romieu-Mourez, D.H. Sherr, G.E. Sonenshein, The RelA NF-kappaB subunit and the aryl hydrocarbon receptor (AhR) cooperate to transactivate the Myc promoter in mammary cells, Oncogene 19 (2000) 5498–5506.
[15] J. Gonçalves, A. Fri3es, L. Moura, Congenital adrenal hyperplasia: focus on the molecular basis of 21-hydroxylase deficiency, Expert Rev. Mol. Med. 9 (2007) 1–23.
[16] T.A. Zimmers, X. Jin, J.C. Gutierrez, C. Acosta, I.H. McKillop, R.H. Pierce, L.G. Koniaris, Effect of in vivo loss of GDF-15 on hepatocellular carcinogenesis, J. Cancer Res. Clin. Oncol. 134 (2008) 753–759.
[17] E.C. Hsiao, L.G. Koniaris, T. Zimmers-Koniaris, S.M. Sebald, T.V. Huynh, S.J. Lee, Characterization of growth-differentiation factor 15, a transforming growth factor beta superfamily member induced following liver injury, Mol. Cell. Biol. 20 (2000) 3742–3751.
[18] S. Svegliati, R. Cancello, P. Sambo, M. Luchetti, P. Paroncini, G. Orlandini, G. Discepoli, R. Paterno, M. Santillo, C. Cuozzo, S. Cassano, E.V. Avvedimento, A. Gabrielli, Platelet-derived growth factor and reactive oxygen species (ROS) regulate Ras protein levels in primary human fibroblasts via ERK1/2. Amplification of ROS and Ras in systemic sclerosis fibroblasts, J. Biol. Chem. 280 (2005) 36474–36482.
[19] J.W. Tullai, M.E. Schaffer, S. Mullenbrock, S. Kasif, G.M. Cooper, Identification of transcription factor binding sites upstream of human genes regulated by the phosphatidylinositol 3-kinase and MEK/ERK signaling pathways, J. Biol. Chem. 279 (2004) 20167–20177.
[20] A.J. Kudla, M.L. John, D.F. Bowen-Pope, B. Rainish, B.B. Olwin, A requirement for fibroblast growth factor in regulation of skeletal muscle growth and differentiation cannot be replaced by activation of platelet-derived growth factor signaling pathways, Mol. Cell. Biol. 15 (1995) 3238–3246.
[21] P.A. Bromann, H. Korkaya, C.P. Webb, J. Miller, T.L. Calvin, S.A. Courtneidge, Platelet-derived growth factor stimulates Src-dependent mRNA stabilization of specific early genes in fibroblasts, J. Biol. Chem. 280 (2005) 10253–10263.
[22] L. Rahib, N.K. MacLennan, S. Horvath, J.C. Liao, K.M. Dipple, Glycerol kinase deficiency alters expression of genes involved in lipid metabolism, carbohydrate metabolism, and insulin signaling, Eur. J. Hum. Genet. 15 (2007) 646–657.
[23] A.A. Toye, L. Moir, A. Hugill, L. Bentley, J. Quarterman, V. Mijat, T. Hough, M. Goldsworthy, A. Haynes, A.J. Hunter, M. Browne, N. Spurr, R.D. Cox, A new mouse model of type 2 diabetes, produced by N-ethyl-nitrosourea mutagenesis, is the result of a missense mutation in the glucokinase gene, Diabetes 53 (2004) 1577–1583.